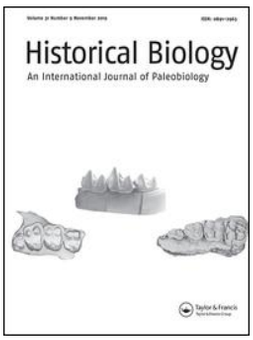

Historical Biology

An International Journal of Paleobiology

ISSN: 0891-2963 (Print) 1029-2381 (Online) Journal homepage: https://www.tandfonline.com/loi/ghbi20

A revision of the referred specimen of *Chuanjiesaurus anaensis* Fang et al., 2000: a new early branching mamenchisaurid sauropod from the Middle Jurassic of China

Xin-Xin Ren, Toru Sekiya, Tao Wang, Zhi-Wen Yang & Hai-Lu You

To cite this article: Xin-Xin Ren, Toru Sekiya, Tao Wang, Zhi-Wen Yang & Hai-Lu You (2020): A revision of the referred specimen of *Chuanjiesaurus anaensis* Fang et al., 2000: a new early branching mamenchisaurid sauropod from the Middle Jurassic of China, Historical Biology, DOI: 10.1080/08912963.2020.1747450

To link to this article: https://doi.org/10.1080/08912963.2020.1747450

Published online: 09 Apr 2020.

HISTORICAL BIOLOGY
https://doi.org/10.1080/08912963.2020.1747450

Taylor & Francis
Taylor & Francis Group

ARTICLE

A revision of the referred specimen of *Chuanjiesaurus anaensis* Fang et al., 2000: a new early branching mamenchisaurid sauropod from the Middle Jurassic of China

Xin-Xin Ren[a,b,c], Toru Sekiya[d], Tao Wang[e], Zhi-Wen Yang[e] and Hai-Lu You[a,b,c]

[a]Key Laboratory of Vertebrate Evolution and Human Origins, Institute of Vertebrate Paleontology and Paleoanthropology, Chinese Academy of Sciences, Beijing, China; [b]CAS Center for Excellence in Life and Paleoenvironment, Beijing, China; [c]College of Earth and Planetary Sciences, University of Chinese Academy of Sciences, Beijing, China; [d]Fukui Prefectural Dinosaur Museum, Katsuyama City, Japan; [e]Bureau of Land and Resources of Lufeng County, Yunnan Province, China

ABSTRACT

We present a revision of the referred specimen (LFGT LCD 9701–1) of *Chuanjiesaurus anaensis* from the Middle Jurassic Chuanjie Formation of Yunnan Province, southwest China, and demonstrate that LCD 9701-1 is differentiated from the holotype by numerous features. Therefore, it can be referred to a new taxon (*Analong chuanjieensis* gen. et sp. nov.). *Analong* bears a unique combination of characters, such as caudal transverse processes persisting until the 10th caudal (15th in *Chuanjiesaurus*); weakly developed posterior condylar ball in anterior caudal vertebrae (well developed in *Chuanjiesaurus*); ulnar anterolateral and anteromedial processes sub-equal in length and forming an angle of about 45 degrees (unequal in length and 60 degrees in *Chuanjiesaurus anaensis*); proximal width of metacarpal II 7% the length of radius (lowest value among mamenchisaurids); pubic distal width approximately 40% of its total length (greatest value among mamenchisaurids). Comparative study and cladistic analysis show *Analong chuanjieensis* is the earliest branching of Mamenchisauridae, while the (*Mamenchisaurus* + *Chuanjiesaurus anaensis*) branching is the latest branching of this clade. Our revision of *Analong chuanjieensis* increases the diversity of Mamenchisauridae and indicates the evolution of Mamenchisauridae is a complex than previously realised.

ARTICLE HISTORY
Received 20 January 2020
Accepted 23 March 2020

KEYWORDS
Chuanjie; Yunnan; middle Jurassic; Chuanjie Formation; Mamenchisauridae; *Analong*

Introduction

Sauropod dinosaurs were gigantic long-necked herbivorous dinosaurs that dominated many Jurassic and Cretaceous terrestrial faunas (Upchurch et al. 2004). The Early-Middle Jurassic was a critical period in the early evolution of sauropods, with the decline of basal sauropodomorphs and the appearance of the early diverging sauropods (e.g. Wang et al. 2017; Zhang et al. 2018; Yates and Kitching 2003; Upchurch et al. 2004; 2007; Allain and Aquesbi 2008; Cúneo et al. 2013), including the initial radiation of eusauropods (e.g. Bonaparte 1986; Zhang 1988; He et al. 1998; Ouyang and Ye 2002; Upchurch and Martin 2003; Bandyopadhyay et al. 2010). China is well known for its diverse array of eusauropod dinosaurs from the Middle Jurassic horizons such as the Lower Shaximiao Formation (e.g. Dong et al. 1983; Zhang 1988; Ouyang 1989; Pi et al. 1996; He et al. 1998; Peng et al. 2005; Xing et al. 2015b), but there are still a large number of potential contributions from the Chinese record that remain under-exploited and are valuable to gain an understanding of basal sauropod evolution (McPhee et al. 2016). Besides abundant basal sauropodomorph materials from the Lower Jurassic (Young 1941, 1942, 1947, 1948, 1951; Zhang and Yang 1995; Lü et al. 2010; Sekiya and Dong 2010; Wang et al. 2017; Zhang et al. 2018), the Lufeng Basin of Yunnan Province also yields Middle Jurassic sauropods (Fang et al. 2004; Sekiya 2011).

Fang et al. (2000) described an assemblage of material from a quarry in the Middle Jurassic Chuanjie Formation in the Lufeng World Dinosaur Valley, close to the town of Konglongshan, Lufeng Country in Yunnan Province, provided the name *Chuanjiesaurus anaensis* for this material, and interpreted it as a member of Cetiosauridae. Sekiya (2011)'s re-examination suggested that this assemblage was composed of at least two individuals (a holotype and a referred specimen), and through cladistic analysis found *Chuanjiesaurus* belongs to Mamenchisauridae. Its mamenchisaurid affinity has since been confirmed by other studies (Xing et al. 2015b; Ren et al. 2018). However, based on our re-examination, the holotype and referred specimen possess numerous differences. Here we provide a detailed description of the referred specimen, compare it to the holotype and other related taxa, and perform a cladistic analysis to reveal its affinity.

Systematic palaeontology

Dinosauria (Owen 1842)
Saurischia (Seeley 1887)
Sauropodomorpha (Huene 1932)
Sauropoda (Marsh 1878)
Eusauropoda (Upchurch 1995)
Mamenchisauridae (Young and Chao 1972)

Analong chuanjieensis gen. et sp. nov. (Figure 2–4)

Holotype. Lufeng World Dinosaur Valley: LFGT LCD9701-1. Some records employed 9701-I, the 'I' is the Greek word, meaning one. The specimen is still preserved *in-situ* for exhibition at Lufeng Dinosaur Valley. The holotype preserves 11 articulated cervical vertebrae (axis – cervical 12), 8 middle-posterior dorsal vertebrae, 4 or 5 sacral vertebrae, first 24 caudal vertebrae, and chevrons, some dorsal ribs, pubes and individually specify that the humerus, ulna, radius, metacarpals, ilium and femur are all from the left side.

Etymology. The generic name refers to the village where the holotype was found; 'long' means dragon in Chinese Pinyin. The specific name refers to the town that the village belongs to.

CONTACT Xin-Xin Ren laotourenxin@126.com 142 Xizhimenwai Street, Beijing 100044, China

Published online 09 Apr 2020

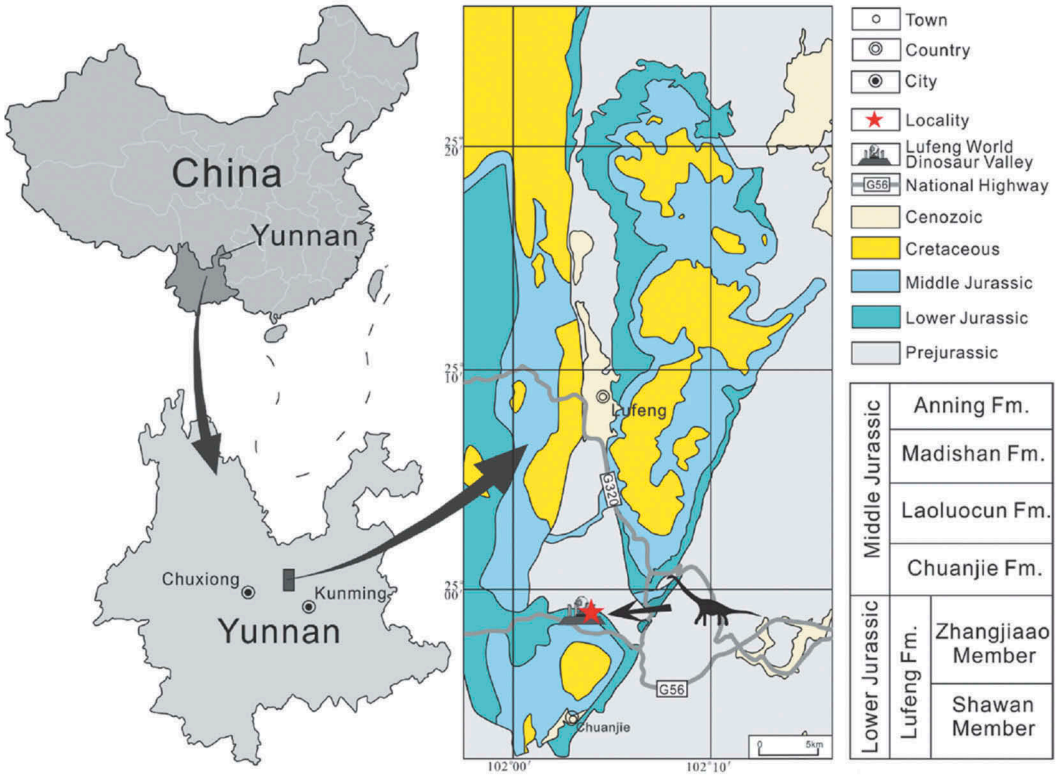

Figure 1. Geographic and geological maps showing the location of *Analong chuanjieensis* gen. et sp. nov. (indicated by the red star), and generalised stratigraphic section of Early and Middle Jurassic in Lufeng Basin, modified from Fang et al. (2000)

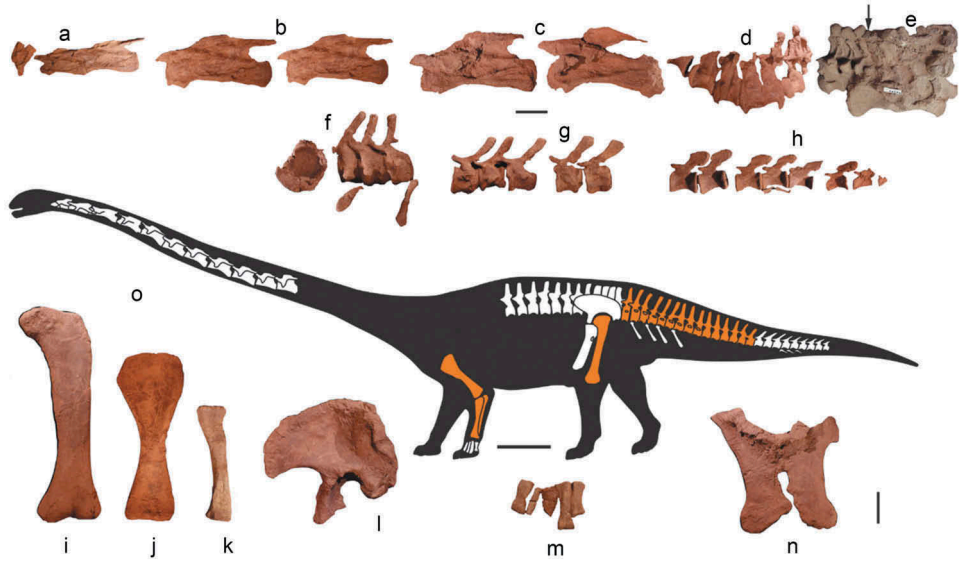

Figure 2. Representative elements of *Analong chuanjieensis* gen. et sp. nov. and reconstruction of the skeleton. (A) Anterior cervical vertebrae (2–4). (B) Middle cervical vertebrae (8, 9). (C) Last preserved two middle cervical vertebrae (11, 12). (D) Articulated five middle – posterior dorsal vertebrae. (E) Last three dorsal vertebrae and sacral vertebrae (1–4). (F) Anterior caudal vertebrae (1–4). (G) Anterior caudal vertebrae (7–11). (H) Middle caudal vertebrae (18–24). (A – H) Left lateral views, and caudal 1 in anterior view in F. (J) Left humerus in anterior view. (K) Left radius in medial view. (M) Left metacarpals in dorsal views. (L) Left ilium in lateral view. (N) Articulated pubes in ventral view. (I) Left femur in anterior view. (O) Reconstruction of the skeleton of *Analong chuanjieensis* gen. et sp. nov. in left lateral view, the elements in orange are also preserved in the holotype of *Chuanjiesaurus anaensis* (the left femur mirrored). Arrow shows the 1st sacral. Scale bars equal 20 cm in A – N, and 1 m in O.

Diagnosis

A mamenchisaurid eusauropod possessing the following unique combination of character states (autapomorphies are marked by *): caudal transverse processes persisting until the 10th caudal* (*Chuanjiesaurus anaensis*: 15th); weakly developed posterior condylar ball in anterior caudals (*Chuanjiesaurus anaensis*: well developed); bifid chevrons in middle caudal series; length of ulnar proximal condylar processes sub-equal (*Chuanjiesaurus*

anaensis: unequal); angle between the ulnar anterolateral and anteromedial processes about 45 degrees* (*Chuanjiesaurus anaensis*: 60 degrees); proximal width of metacarpal II is 7% the length of radius (lowest value among mamenchisaurids)*; distal width approximately 40% of the total length of the pubis (greatest value among mamenchisaurids)*.

Locality and horizon

The specimen was excavated near A'na Village, Chuanjie Town (now Konglongshan Town), Lufeng County, Chuxiong Yi Autonomous Prefecture, Yunnan Province, southwest China (Figure 1). The specimen was recovered from the base of the Chuanjie Formation, which is composed of purplish red silty mudstones. The base of the Chuanjie Formation was regarded to be Middle Jurassic (Bajocian), according to the magnetostratigraphic study of Huang et al. (2015).

Description

Cervical vertebrae

(axis to 12th) articulated cervical vertebrae are preserved in situ. They are mostly intact with the left side exposed (Figures 2–3; Figs 5–14 (Sekiya (2011)); see Table 1 from Sekiya (2011) for measurements). Rather than fully describing the anatomical features of each vertebra, we divided the cervical series into two parts, and document changes along the sequence. The axis to Ca 5 is presumed as anterior series. Ca 6–12 are prominently elongate with lengths of their centra nearly equal, therefore, they are presumed as middle series (referred Tschopp et al. (2015), see Table 3 of that study). All centra are opisthocoelous.

Anterior cervical vertebrae

The anterior articular surfaces of centra are generally convex and the posterior ones are shallowly concave. The ventral surfaces are

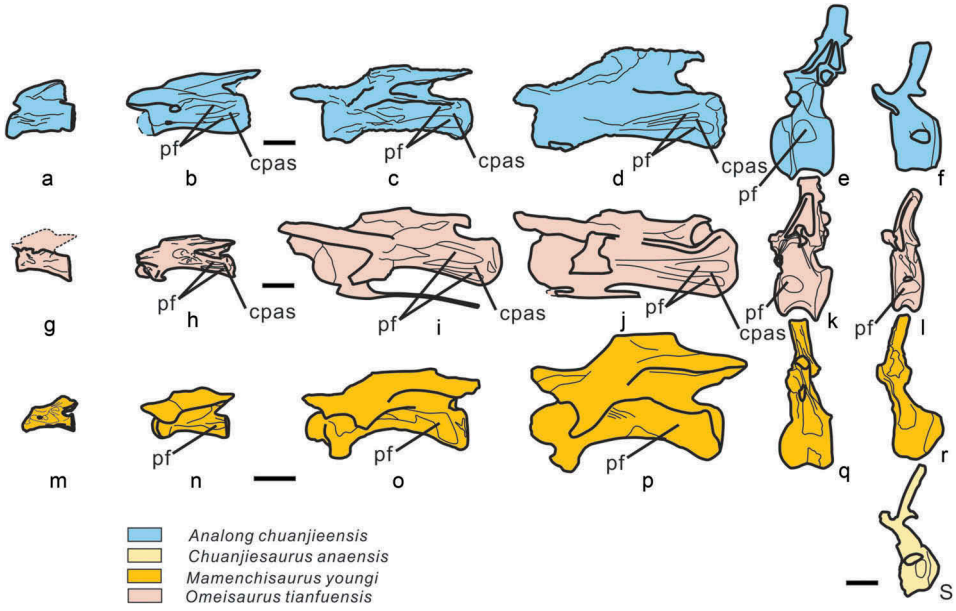

Figure 3. Comparison of selected vertebrae of *Analong chuanjieensis* (A – F), *Omeisaurus tianfuensis* (G – L), *Mamenchisaurus youngi* (M – R) and *Chuanjiesaurus anaensis* (S) in left lateral views. (A) Axis. (B) Ca 3. (C) Ca 8. (D) Ca 12. (E) Last dorsal vertebra. (F) Cd 3. (G) Axis. (H) Ca 3. (I) Ca 8. (J) Ca 12. (K) D 7. (L) Cd 3. (M) Atlas and axis. (N) Ca 3. (O) Ca 8. (P) Ca 12. (Q) D 7. (R) Cd 3. Scale bars equal 10 cm. Abbreviations: ca, cervical; cd, caudal; d, dorsal; pf, pneumatic fossa or foramen.

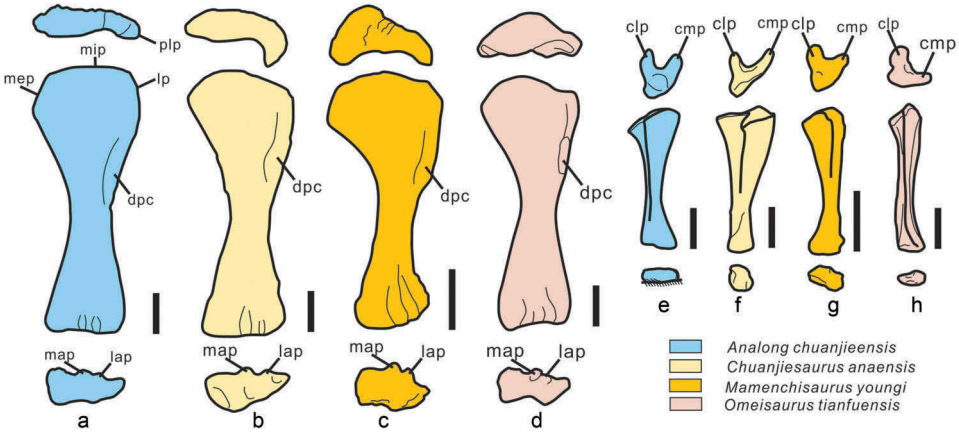

Figure 4. Comparison of forelimbs of *Analong chuanjieensis* (A and E), *Chuanjiesaurus anaensis* (B and F), *Mamenchisaurus youngi* (C and G) and *Omeisaurus tianfuensis* (D and H). (A, B and D) Left humerus. (C) Right (left in reverse) humerus. (E, G and H) Left ulna. (F) Right (Left in reverse) ulna. Humeri are arranged from top to bottom in proximal in proximal, anterior and ventral views, Ulnae are arranged from top to bottom in proximal, lateral and ventral views. Abbreviations: clp, anterolateral process; cmp, anteromedial process; dpc, deltopectoral crest; lap, lateral accessary process; map, medial accessary process; mep, medial part of proximal surface mip, middle part of proximal surface; lp, lateral process; plp, proximolateral process.

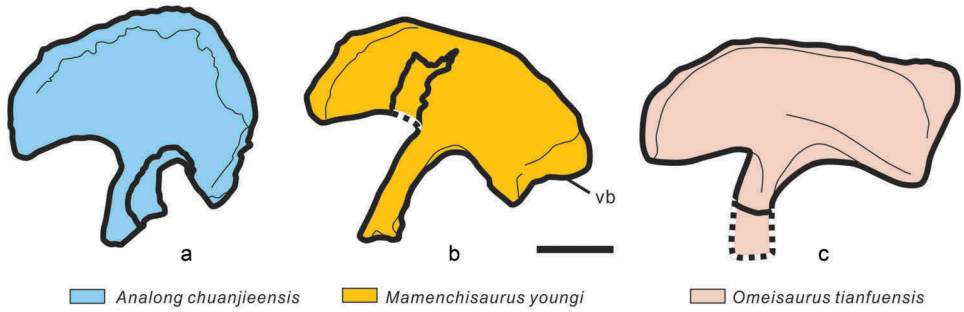

Figure 5. Comparison of ilia of *Analong chuanjieensis* (A), *Mamenchisaurus youngi* (B) and *Omeisaurus tianfuensis* (C) in lateral views. (A and C) Left ilium. (B) Right (Left in reverse) ilium. Dashed lines indicated missing bone. Scale bars equal 20 cm. Abbreviation: vb, ventral bulge.

Table 1. Selected ratios for forelimb elements of some mamenchisaurids.

Taxon	HRI	URP	URL	URM	Specimen and/or source
Omeisaurus tianfuensis	0.28	85	0.21	0.21	T5701, He et al. 1998
Omeisaurus maoianus	0.28	–	0.32	0.24	N8510, Tang et al. 2001
Omeisaurus jiaoi	–	–	0.24	–	ZDM5050, Jiang et al. 2011
Anhuilong diboensis	0.26	85	0.31	0.44	AGB 5822, Ren et al. 2018
Huangshanlong anhuiensis	0.27	75	0.38	0.46	AGB 5818, Huang et al. 2014
Chuanjiesaurus anaensis	0.29	60	0.25	0.40	Lfch 1001, Fang et al. 2000
Analong chuanjieensis	0.29	45	0.35	0.30	LCD 9701–1, This paper
Mamenchisaurus youngi	0.29	58	0.28	0.32	ZDM 0083, Ouyang and Ye 2002
Mamenchisaurus jingyanensis	0.34?	–	–	–	CV 00734, Zhang et al. 1998

The URP measured the angle between the long-axes of the anteromedial and anterolateral processes; URL measured from the posterior surface to the tip of the anterolateral process; URM measured from the posterior surface to the tip of the anteromedial process. Abbreviations: hri, the average of the greatest widths of the proximal end, mid-shaft and distal end of humerus/length of humerus; urp, angle between anterolateral and anteromedial processes of ulna; url, ratio of length of anterolateral process to total length of ulna; urm, ratio of length of anteromedial process to total length of ulna.

broad and mostly flat without ventral midline keel. The ventrolateral ridges of the centra are obvious except on the axis, and that on the axis is absent. The length/posterior articular surface height ratios of the anterior cervical centra range from 2.2 to 2.6, and these values are larger than that in *Shunosaurus lii* (1.7–2.3) (Zhang 1988), but are much less than the values of *Omeisaurus tianfuensis* (2.9–3.9) (He et al. 1998). Pneumatic fossae exist on the lateral surfaces. Two elliptical pneumatic fossae are located on the posterior half of the lateral surface of axial centrum, and the anteroventral one is slightly deeper than the posterior one. A big fossa is on the anterior portion of other anterior cervical centra and another two fossae on the posterior portion, divided by an accessory septum (Figure 3, cpas). This septum slightly anteroventrally directed, producing posteroventral and anterodorsal portions of the centrum. This pneumatic morphology is similar to that of *Omeisaurus tianfuensis*, but the fossae are much shallower than that in *Omeisaurus tianfuensis*, and this character is different in other taxa such as *Mamenchisaurus youngi*. The parapophyses are broad, and the anteroposterior length is about 15% the total length of centra. They extend ventrally beyond the ventral level of the centrum, about 20% the height of centra. The shape of parapophyses is elliptical mostly. Posteriorly the parapophyses merged smoothly with the ventrolateral ridges of the centra.

The neural arches are prominently shorter than the centra, potentially reaching the ratio about 0.5, and approximately equal to the height of neural spines. It is similar to that of *Omeisaurus tianfuensis*. The prezygapophyses extend beyond the centra and are supported by the transversely thin centroprezygapophyseal lamina (CPRL), which seems to merge with prezygodiapophyseal lamina (PRDL) posteroventrally. The CPRL is not divided, connecting intraprezygapophyseal lamina (TPRL) by the ventral of prezygapophysis. Moreover, a deep and long cavity is bounded by the CPRL and TPRL. These laminae also exist in *Omeisaurus tianfuensis* (He et al. 1998), but they are absent in *Shunosaurus lii* (Zhang 1988). The diapophyses are situated on the neurocentral junction at the vertical level of the anterior edge of the neural spine. They are fused with the tuberculum and form a broad ventrolateral extension. The posterior centrodiapophyseal lamina (PCDL) weakly developed, similar to that in *Shunosaurus lii* (Zhang 1988) and *Omeisaurus tianfuensis* (He et al. 1998), whereas these lamina are prominent in *Mamenchisaurus youngi* (Ouyang and Ye 2002). The postzygodiapophyseal lamina (PODL) is prominent, resembling that in most sauropods. The postzygapophyses extend beyond the centra. The epipophysis is a slightly convex tubercle with a coarse surface, which is on the middle portion of dorsal surface of each postzygapophysis. The articular facets of postzygapophyses are concave and face ventrolaterally. The centropostzygapophyseal lamina (CPOL) is a single element and extends ventromedially.

The neural spines are short, more than one fourth the length of the centra. They are dorsoventrally low and transversely narrow and keep this depth and narrowness along the whole length of the neural spine. The spinoprezygapophyseal lamina (SPRL) and the spinopostzygapophyseal lamina (SPOL) start from the base of the neural spine, resembling most sauropods such as *Omeisaurus tianfuensis*.

Middle cervical vertebrae

Both the anterior and posterior articular surfaces are taller than wide, according to the curvature of half exposed portion. Based on the exposed portion, the highest average elongation index value (aEI) is below four (3.4), and the length of the longest centrum/the height of posterior articular surface is also below four (3.9). This feature resembles that in some sauropod taxa such as *Tazoudasaurus naimi* (Allain and Aquesbi 2008), *Shunosaurus lii* (Zhang 1988), *Barapasaurus tagorei* (Bandyopadhyay et al. 2010), *Cetiosaurus oxoniensis* (Upchurch and Martin 2003), *Patagosaurus fariasi* (Bonaparte 2002), and *Mamenchisaurus youngi* (Ouyang and Ye 2002), but different from some taxa with the value greater than four (e.g. *Omeisaurus tianfuensis* (He et al. 1998)). The ventrolateral ridges of the centra are obvious. The ventral surfaces are slightly concave transversely through their whole length and both ends are flat. The midline keel is absent. The entire lateral surfaces are concave and within a big fossa, a sub-fossa and an additional one posterior to it occupy almost of the posterior three fourths portion of this big fossa. Generally, this pneumatic morphology is similar to

that of the anterior series but with slightly more laminae dividing the fossae, a similar condition is also present in *Omeisaurus tianfuensis*, but *Omeisaurus tianfuensis* possesses more complex and deeper pneumatic fossae. Comparing with some taxa of *Omeisaurus* (e.g. Tan et al. 2018; He et al. 1998), *Analong* also share a large anteroposteriorly extended concavity on the lateral surface of middle cervical centrum. An accessory septum slightly anteroventrally directed, producing posteroventral and anterodorsal portions of the centrum, similar to that in *Omeisaurus tianfuensis*. On the central part of the lateral fossa, some secondary septa exist on the anterior part of the big fossa and divide the big fossa into more secondary fossae, resembling *Omeisaurus tianfuensis* and *Omeisaurus* sp. whereas there are more secondary septa and secondary fossae in *Omeisaurus tianfuensis* and *Omeisaurus* sp. (2018; He et al. 1998). The diapophysis – tuberculum region extends ventrolaterally beyond the dorsal level of the centrum, and the parapophysis – capitulum region extends ventrolaterally well below the ventral level of the centrum. They are broad and within the anterior half of the centra. The posterior of the parapophyses merge smoothly with the ventrolateral ridge of the centra.

The neural arches are significantly taller than the neural spines. They are situating along the centra except for the portion ventral to the prezygapophyese and postzygapophyses. In posterior view, the neural canal is small and wider transversely than the dorsoventral height. Ventrally, the prezygapophysis is supported by the transversely thin centroprezygapophyseal lamina (CPRL), and merges with prezygadiapophyseal lamina (PRDL) posteriorly. CPRL is divided and its dorsal edge merges the intraprezygapophyseal lamina (TPRL) which meets its dorsal to the neural canal. A deep and long cavity (CPRF) is bounded by the CPRL and TPRL. The diapophyses are situated on the neurocentral junction at the vertical level along the anterior edge of the neural spines, resembling that in *Omeisaurus tianfuensis* (He et al. 1998) and *Mamenchisaurus youngi* (Ouyang and Ye 2002). The posterior centrodiapophyseal lamina (PCDL) is prominent, similar to that in *Omeisaurus tianfuensis* (He et al. 1998). No distinct lateral fossa exists on the prezygapophysis process, whereas this feature exists in *Omeisaurus tianfuensis* (He et al. 1998), *Mamenchisaurus youngi* (Ouyang and Ye 2002), *Apatosaurus ajax* (Upchurch et al. 2004), *Europasaurus holgeri* (Carballido and Sander 2013), *Brachiosaurus altithorax* (Taylor 2009), and *Amargasaurus cazaui* (Salgado and Bonaparte 1991). The articular surface of prezygapophysis is broad and ventrolaterally extended. The postzygodiapophyseal lamina (PODL) is prominent and consists of the dorsal and anterior parts of the postzygapophyseal centrodiapophyseal fossa (pocdf), resembling that in most sauropods such as *Omeisaurus tianfuensis* (He et al. 1998). The anterior half of the pocdf is more deeply excavated than the posterior half with wrinkled surface texture. The postzygapophyses of each vertebrae slightly extend beyond each centrum except for Ca 10 to Ca 12. Its articular facet is concave and faces ventrolaterally and posteriorly. The postzygapophyses of previous vertebra are articulated with the next prezygapophyses, as a result, the medial parts of the laminae of the postzygapophysis such as the centropostzygapophyseal lamina (CPOL) and intrapostzygapophyseal lamina (TPOL) are invisible.

The neural spines anteroposteriorly elongate prominently, about half the length of the centra. It is dorsoventrally low, transversely narrow, keeps this depth and narrowness along its whole length. The spinoprezygapophyseal lamina (SPRL) is not well preserved and starts from the base of the neural spine. The spinopostzygapophyseal lamina (SPOL) starts from the posterodorsal corner of the neural spine and projects posterolaterally with its dorsal edge along almost the entire length of the postzygapophysis.

Middle to posterior dorsal vertebrae

Eight dorsal vertebrae are preserved and loosely articulated *in-situ* and Sekiya (2011) suggested that there are seven dorsals at least, we rechecked the specimen and believe that the first dorsosacral vertebra in the previous paper by Sekiya (2011) is the last dorsal vertebrate, therefore, there are eight dorsals in this description. Most of them are partly preserved, only six centra of vertebrae are well preserved and visible (the first to the sixth in Figure 2D; the sixth to eighth in Figure 2E; Figs 16–18 (Sekiya (2011)); see Table 2 from Sekiya (2011) for measurements). Since the last two centra are invisible the measurements only include the first six vertebrae and they are numbered from anterior to posterior (Sekiya 2011). The centra are opisthocoelous, with hemispheric convex anterior surfaces and deep concave posterior surfaces. Both of anterior and posterior articular surfaces are taller than wide, according to the degree of curvature of the exposed surfaces of each centra and fifth (counted from front to back) preserved dorsal vertebrae. The length/posterior surface height ratio of the posterior dorsal centra range from 0.67 to 0.83, resembling that in *Omeisaurus tianfuensis* (about 0.8), different from that in *Shunosaurus lii* (0.7–1.1) and *Mamenchisaurus youngi* (about 0.6). The height/the width of posterior surface in posterior centra are about 1.6; similar to that in *Omeisaurus tianfuensis* (1.5–1.6), and larger than that in *Mamenchisaurus youngi* (about 1.4). The ventral surfaces are narrow and slightly convex transversely, rounding smoothly into the lateral surfaces with no distinct ridges, similar to most sauropods such as *Barapasaurus tagorei, Patagosaurus fariasi, Shunosaurus lii, Omeisaurus tianfuensis*, and *Mamenchisaurus youngi* (Bonaparte 1986; Zhang 1988; He et al. 1998; Ouyang and Ye 2002; Bandyopadhyay et al. 2010). At their anterior portion of centra in anterior view, there is an irregular convexity immediately below the neural canal floor. The posterior articular surfaces are deeply concave in posterior view, similar to *Shunosaurus lii* and *Omeisaurus tianfuensis*. Laterally, a deep pneumatic fossa exists on the anterior portion of the centra, and septa preserve inside the fossa dorsally and ventrally. This septum is low with robust base and anteroposteriorly extended in each persevered dorsal, divided the fossa into two small elliptical secondary fossae. The robust base of the septa is gently curves make the deepest region of each secondary fossa is on the centre, other than near the septa. These septa are absent in most early diverging sauropods such as *Tazoudasaurus naimi* (Allain and Aquesbi 2008), *Shunosaurus lii* (Zhang 1988), *Barapasaurus tagorei* (Bandyopadhyay et al. 2010), *Cetiosaurus oxoniensis* (Upchurch and Martin 2003), and *Patagosaurus fariasi* (Bonaparte 1986), but exist in *Omeisaurus tianfuensis* (He et al. 1998), and *Mamenchisaurus youngi* (Ouyang and Ye 2002).

The neural arches appear to have been relatively short, possibly equal to the height of their respective posterior articular surface or less. The ratio of the height of neural arch to the height of posterior articular surface is below one (e.g. Dn 5 is 0.88; Dn 6 is 0.80), it is lower than that in *Shunosaurus lii* (about 1.6), *Omeisaurus tianfuensis* (1.2). The neural canals are slot-shaped, being considerably taller than wide. The base of the parapophyses lies just under the level of the dorsal extreme of the neural canal. Articular surfaces of the parapophyses are oval. The arch extends well above the top of the neural canal and the middle portion of the arch is shallowly concave. The diapophyses are short, curve smoothly into the dorsal surfaces of the processes. This condition is common in most sauropods such as *Shunosaurus lii* (Zhang 1988) and *Omeisaurus tianfuensis* (He et al. 1998). Orientation of diapophysis is lateral and slightly dorsal, resembling that in *Omeisaurus tianfuensis* (He et al. 1998), *Mamenchisaurus youngi* (Ouyang and Ye 2002), *Barapasaurus tagorei* (Bandyopadhyay et al. 2010), *Apatosaurus ajax* (Upchurch et al. 2004), *Malawisaurus* (Jacobs et al. 1993), *Alamosaurus sanjuanensis* (Gilmore

1946), *Opisthocoelicaudia* (Borsuk-Bialynicka 1977) and *Rapetosaurus krausei* (Curry-Rogers and Forster 2004). The centropostzygapophyseal lamina (CPOL) extends dorsally, from the dorsal opening of the neural canal to the ventrolateral corner of postzygapophysis. The articular surface of prezygapophyses is dorsally oriented. The prezygapophyses appear to have been positioned very close to each other with respect to the midline. A ridge extends backwards from the posterodorsal base of the prezygapophysis, towards to the diapophysis and the base of the neural spine (in the case of the former it would be the prezygodiapophyseal lamina (PRDL), in the latter is the spinoprezygapophyseal lamina (SPRL)). The prezygoparapophyseal lamina (PRPL) orientates 60 degrees to the horizontal, connects the prezygapophysis to the parapophysis. The paradiapophyseal lamina (PPDL) and posterior centroparapophyseal lamina (PCPL) are on the dorsoposterior and anteroventral of parapophysis, respectively. Still, the posterior centrodiapophyseal lamina (PCDL) and spinodiapophyseal lamina (SPDL) are perpendicular to the diapophysis, respectively. The PRPL, PRDL and PCDL surround a deep fossa, and divided by the PPDL in the centre. The deep fossa consisting by prcdf and cdf, situated on anterior and posterior portions, respectively. The postzygodiapophyseal lamina (PODL) is prominent and surrounds the postzygapophyseal centrodiapophyseal fossa (pocdf) anterodorsally. The anterior half of the pocdf is more deeply excavated than the posterior half with coarse surface. The postzygapophyses articular facets are concave and face ventrolaterally and posteriorly. They slightly extend over the centra. The hyposphene-hypantrum system weakly extend under the postzygapophyses with a V-shape, and consisting the posterior portion of pocdf.

The shape of neural spines is plate shaped with a knob-like top. The orientation of the neural spines is vertical, resembling that in early branching sauropods such as *Tazoudasaurus naimi* (Allain and Aquesbi 2008), *Shunosaurus lii* (Zhang 1988) and some advanced taxa (e.g. *Europasaurus holgeri* (Carballido and Sander 2013), *Nigersaurus taqueti* (Sereno et al. 2007)). The height of the neural spines/height of the posterior dorsal vertebrae are about 0.30–0.37, similar to *Omeisaurus tianfuensis* (about 0.3), and the value lower than that in *Shunosaurus lii* (about 0.5). In anterior view, the morphology of neural spines is rectangular for most of its length with no lateral expansion, resembling to most sauropods. The spinoprezygapophyseal lamina (SPRL), spinopostzygapophyseal lamina (SPOL), and spinodiapophyseal lamina (SPDL) are well preserved, and start from the base of the neural spines. The anteroposterior length/transverse width of the top of the neural spines is about 0.8.

Sacral vertebrae

The sacrum consists of four sacral vertebrae (since the poorly-preserved condition and the most anterior of the sacrum might be dorsosacral vertebra. Four neural spines and ribs of the sacrals are clearly identified (see the description below), we are not very sure if any loss for the poor preservation), all of which are preserved in articulation with each other, and all of them are ambiguous with the pelvic elements squashed (Figure 2; Fig. 18 (Sekiya (2011))). Only four distal of sacral neural spines and sacral transverse processes are prominently distinguishable, other portion of each sacrum are buried by surrounding rocks. This four-sacral condition is common in early diverging sauropods (e.g. *Shunosaurus lii, Barapasaurus tagorei*, and *Omeisaurus tianfuensis*) (Zhang 1988, Fig. 34; Bandyopadhyay et al. 2010; He et al. 1998, Figs 31 and 32). Based on their morphology and relative position, the anterior-most element is interpreted as a dorsosacral vertebra with the first obviously dorsoventrally elongated transverse processes different with the previous dorsal series, the middle two elements as primordial sacral vertebrae, and the posterior one as a caudosacral vertebra with the neural spine visible. The first sacral vertebra (dorsosacral) is placed between the anterior end of the pubic peduncle and the acetabulum of the ilium, as the ilium slight misplaced. It seems that the sacral vertebrae are fully fused from the dorsosacral vertebrae to the subsequent ones, but they likely could be compressed during burial. The dorsal surface of sacral ribs seems to lie below the dorsal margin of the ilium. The diapophysis projects posterolaterally, resembling to the morphological features of most basal sauropods. The neural spines of the sacral vertebrae are expanded knob-like quadrate shaped and completely fused each other totally. Maybe the totally fused neural spines partly caused of squash.

Caudal vertebrae

There are 24 caudal vertebrae preserved, counted from the first caudal vertebrae (Figure 2–3; Fig. 20 and Figs 28–35 (Sekiya (2011)); see Table 4 from Sekiya (2011) for measurements). We define the first 15 caudals are the anterior caudal vertebrae and the rest preserved belonging to the middle series (refer to Tschopp et al. (2015)). The centra are solid, the first 13 anterior caudal vertebrae (maybe 15 anterior caudals) are procoelous, and the subsequent ones are amphicoelous or slightly amphiplatyan distally. Anterior caudal centra (Cd 1–Cd 10), anteroposterior length of posterior condylar ball to mean average radius of anterior articular surface of centrum ratio is about 0.27, whereas that in *Omeisaurus tianfuensis* is zero for the amphicoelous articular surfaces, the holotype of *Chuanjiesaurus anaensis* is about 0.37, and that in *Mamenchisaurus youngi* is about 0.91. Lengths of caudal vertebral bodies are basically same over first 20, resembling that in most sauropods except some taxa such as *Tornieria africana* (Remes 2006). The centra are slightly dorsoventrally compressed in cross-section throughout, similar to some early diverging sauropods such as *Vulcanodon karibaensis* (Cooper 1984), *Shunosaurus lii* (Zhang 1988), *Cetiosaurus oxoniensis* (Upchurch and Martin 2003), *Omeisaurus tianfuensis* (He et al. 1998), and *Chuanjiesaurus anaensis* (Fang et al. 2000), whereas that in some taxa are transversely compressed (e.g. *Mamenchisaurus youngi* (Ouyang and Ye 2002)). The ventral surfaces of the anterior centra are convex transversely, no groove, ridge or hollow on the ventral surfaces. There is also no obviously ventrolateral ridge on anterior-most caudal vertebrae, which is similar to that in most sauropods. While, ventrolateral ridges exist in some posterior anterior caudal vertebrae (Cd 11–Cd 14), some taxa also share ventrolateral ridges on their middle caudal vertebra such as *Wintonotitan wattsi* (Poropat et al. 2014), *Andesaurus delgadoi* (Calvo and Bonaparte 1991), *Isisaurus colberti* (Wilson and Upchurch 2003), *Alamosaurus sanjuanensis* (Gilmore 1946), *Opisthocoelicaudia skarzynskii* (Borsuk-Bialynicka 1977), and *Saltasaurus loricatus* (Powell 1992). Compare with that in some early diverging taxa, the ridges in *Analong chuanjieensis* are smoother, and *Chuanjiesaurus anaensis* does not share this character with not ventrolateral ridges on their preserved caudals. The dorsoventral heights of the anterior surfaces are 0.54–1.59 times the anteroposterior length of the centra (Cd 1–Cd 24). The dorsoventral heights of the posterior surfaces are 0.54–1.50 times the anteroposterior length of the centra (Cd 1–Cd 24) (Figure 9D).

The position of the neural arches on the anterior caudal centra (especially on Cd 1–Cd 10) exhibits a strong anterior bias, and the neural arches of subsequent centra are generally extend backward, resembling that of *Omeisaurus tianfuensis* and *Chuanjiesaurus anaensis*. The neural arches are mainly on the centre of the vertebra on last vertebrae of the preserved series, although they remain set back from the anterior margin. The transverse processes exist on the anterior 10 ones, whereas that in *Chuanjiesaurus anaensis* and many other taxa (e.g. *Omeisaurus*

tianfuensis) persisting till the 15th caudal. The left transvers process of 7th caudal is damaged, and ventral surface of the transvers process of 10th caudal is still buried in surrounding rocks. The bases of the transverse processes extend for a short distance onto the lateral surface of the centra and the cross-section is elliptical. The shape of transverse processes is 'wing-like', similar to that in *Chuanjiesaurus anaensis*, and *Omeisaurus tianfuensis* (He et al. 1998; Sekiya 2011). The transverse process is laterally and slightly ventrally orientated, and this condition is common in most sauropods (e.g. *Tazoudasaurus naimi, Chuanjiesaurus anaensis, Omeisaurus tianfuensis, Camarasaurus lewisi, Isisaurus colberti*, and *Amargasaurus cazaui*), whereas it curves anteriorly towards its distal end on caudal 8. The prezygapophyses are narrowly spaced, and steeply inclined on the anterior series (the angle of the articular facets to horizontal is about 60 degrees), whereas the angle on the subsequent ones generally decrease (about 45 degrees on the last ones). Lamination of the caudal vertebra is poorly developed, as in other early diverging sauropods. Only the prezygodiapophyseal laminae (PRDL) and the spinoprezygapophyseal lamina (SPRL) exist in anterior caudal vertebrae. PRDL is single, similar to that in most sauropods. SPRLs are small short ridges that rapidly fade out into the anterolateral margin of the spine.

The neural spines are posterodorsally orientated. The neural spines of anterior caudal vertebrae are rod-like, and quadrangle in cross-section. The anteroposterior length generally increases on the subsequent ones, and the shape also generally change to plate-like in lateral view. The height of neural spine/the height of centra of anterior caudal vertebrae are below one (about 0.9).

Chevrons

Seven chevrons are preserved, including four anterior ones (the second and fourth to sixth) and three middle ones (the fourteenth to sixteenth) with left side exposed (Figure 2; Figs. 27, 28, 32 and 34 (Sekiya (2011)); see Table 4 from Sekiya (2011) for measurements).

The expanded proximal ends of the haemal arches (all seven chevrons) form a continuous bridge of bone over the haemal canal, this plesiomorphic condition exists in most early diverging sauropods. The left and right articular surfaces are mildly concave transversely and convex anteroposteriorly in the anterior ones, with the long-axis of the haemal arch held vertically. Anterior parts of facets are smaller than the posterior parts in the anterior ones.

The haemal canal of anterior chevrons is visible, and that in the middle series are invisible for they are still buried in surrounding rocks. The haemal canals are dorsoventrally elongate ellipses in anterior view. It is relatively short compared to the total length of the chevron (about 20% of chevron length in the anterior ones). The left and right rami are transversely compressed with slightly convex medial surface and more strongly convex lateral surfaces. The canal merges with grooves that extend on to the anterior and posterior margins of the distal blade ventrally.

The distal blade of each anterior chevron is broad and rounded with prominently expanded posterior margins, although it narrows transversely towards the distal tip. The middle ones are anteriorly and posteriorly expand and bifurcated into anterior and posterior processes. The posterior processes are more extended than the anterior ones among middle chevrons. Both of processes are slightly ventrally oriented with rounded margins.

Humerus

The left humerus is well preserved *in-situ* (Figures 2 and 4; Fig. 39 (Sekiya (2011)); see Table 6 from Sekiya (2011) for measurement, the distal width and middle least transverse width in Sekiya (2011) need be interchanged). The outline is similar to other mamenchisaurids, the HRI value is 0.29 (Table 1). In anterior view, the proximal and distal portions expand gradually towards both ends, and the medial portion appears to be positioned medial to the middle of the proximal articular surface compare with the lateral portion, giving the proximal end a fan-like shape in anterior view. The proximal width is 40% of total length of the humerus, resembling that in other mamenchisaurids such as *Huangshanlong anhuiensis* (Young 1939; Zhang et al. 1998; He et al. 1998; Tang et al. 2001; Ouyang and Ye 2002; Huang et al. 2014). The humeral head is located at the middle of the proximal end and extends posteriorly in lateral view. In anterior view, the proximal surface of the humerus could be divided into three planes, the lateral, middle and medial, and the middle plane is much longer than other two planes (Figure 2, lp; mip; mep). Compare with other taxa, this 'three plane' character is common in *Shunosaurus lii*, many mamenchisaurids, *Turiasaurus riodevensis*, and some derived neosauropod forms such as *Tornieria africana* and *Saltasaurus loricatus* (Zhang 1988; He et al. 1998; Tang et al. 2001; Ouyang and Ye 2002; Remes 2006; Royo-Torres et al. 2006). Supracoracoideus tuberculum is lacking on the proximolateral portion of the humerus, while it exists in some neosauropods such as *Suuwassea emiliae, Opisthocoelicaudia skarzynskii, Isisaurus colberti*, and *Saltasaurus loricatus* (Royo-Torres et al. 2006; Harris 2006a; Whitlock and Harris 2010).

The ratio of extended length of the deltopectoral crest/total length of humerus is about 0.46 (*Omeisaurus tianfuensis* is 0.44) (distance from proximal end of humerus to most prominent point of deltopectoral crest divided by humerus proximodistal length). It is orientated anteromedially, a similar condition is also present in other early diverging eusauropods (e.g. *Shunosaurus lii, Omeisaurus tianfuensis, Mamenchisaurus youngi, Barapasaurus tagorei*, and *Patagosaurus fariasi*). The cross section of the mid-shaft is ovoid, similar to that in *Vulcanodon karibaensis, Shunosaurus lii, Omeisaurus tianfuensis* and *Huangshanlong anhuiensis* (Cooper 1984; Zhang 1988; He et al. 1998; Huang et al. 2014). The ratio of the width of the cross section to the total length of the humerus is 0.15, which is similar to *Omeisaurus tianfuensis* (0.17).

The distal end is quadrilateral, and the two condyles are convex slightly with coarse surfaces, whereas the shape of humeral distal end of *Chuanjiesaurus anaensis* is cone-like. The anteromedial process is larger than the anterolateral one, *Chuanjiesaurus anaensis* and *Omeisaurus tianfuensis* also share this character. In ventral view, the shape of the distal end of *Analong* is close to a right triangle with more robust medial condyle, whereas that of *Chuanjiesaurus* is close to an obtuse triangle. There are two small accessary processes on the anterodistal edge of the humerus, as in other mamenchisaurids, *Patagosaurus fariasi*, and *Apatosaurus ajax*. Both of the processes are nearly triangular. Additionally, the medial accessory process is more robust than the lateral one, which is similar to that in most mamenchisaurids, except for *Anhuilong diboensis* (Ren et al. 2018). The anconeal fossa is shallow on the posterodistal portion of the humerus, and two processes are semi-round in posterior view.

Ulna

The left ulna is well preserved in situ (Figures 2 and 4; Fig. 41 (Sekiya (2011)); see Table 6 from Sekiya (2011) for measurements, the values on ulnar and radial distal width of holotype (*Chuanjiesaurus anaensis*) need be interchanged). The ulna is slightly longer than the radius, and the ratio of ulnar length to radial length is 1.06 (*Chuanjiesaurus anaensis* is 1.10). The length

of ulna is 0.67 the length of the humerus, this value is approximately similar to other mamenchisaurids (referred Ren et al. 2018, Table, p. 3). The proximal end is triradiate, this condition also exists in other sauropods. The anterolateral and anteromedial processes are prominent and robust, which together in proximal view make up a 'U' shape and form a deep anterior groove that receives the proximal end of the radius. The angle between the two processes (URP) is 45 degrees, which is much small than that in *Chuanjiesaurus anaensis* (60 degrees) (Table 1). It is also smaller than that in other mamenchisaurids such as *Omeisaurus tianfuensis* (about 85 degrees) and *Huangshanlong anhuiensis* (about 75 degrees). The length of the anteromedial process is 0.9 times that of the anterolateral process, that in *Chuanjiesaurus anaensis* is 1.67, and *Omeisaurus tianfuensis* is about 1.0. The posterior process is weakly developed, and the olecranon process is also weak. Along the anterolateral process, the maximum length is 35% of the total length of the ulna, and along the anteromedial process, the maximum length is 30% of the total length of the ulna (*Chuanjiesaurus anaensis* is 25% and 40% respectively; *Omeisaurus tianfuensis* is 21% and 21%, respectively) (Table 1).

The 'U' shape of the proximal surface is transformed into a circular cross section at mid-shaft, resembling that in majority of sauropods such as in *Mamenchisaurus youngi*, but *Chuanjiesaurus anaensis, Huangshanlong anhuiensis, Anhuilong diboensis, Vulcanodon karibaensis*, and *Rapetosaurus kiausei* have an elliptical cross section. On the anterolateral surface of the proximal portion, there is a raised coarse area that matches a similar area on the surface of the radius.

The distal surface of the ulna is oval, and the anterior part is a little flat. By contrast, the shape of the corresponding region in *Omeisaurus tianfuensis* is more compressed, and those of *Chuanjiesaurus anaensis* and *Mamenchisaurus youngi* share a subquadrilateral shape. The maximum length of the distal end is 26% of the total length, much bigger than that in *Chuanjiesaurus anaensis* (0.17). The distal portion of the anteromedial surface is slightly convex where it received the posteromedial surface of the distal end of the radius. *Chuanjiesaurus anaensis, Vulcanodon karibaensis, Omeisaurus tianfuensis*, and *Mamenchisaurus youngi* also share this character. The surface of the distal end is nearly flat, with the centre a little convex. The distal surface is nearly perpendicular to the shaft, similar to that in *Chuanjiesaurus anaensis*. The angle is below 80 degrees in *Omeisaurus tianfuensis, Apatosaurus ajax*, and *Amargasaurus cazaui* (Salgado and Bonaparte 1991; He et al. 1998; Upchurch et al. 2004).

Radius

The left radius is well-preserved and complete *in-situ* (Figures 2 and 6, Fig. 43 in Sekiya (2011) (A in Figs 42 and 43 in Sekiya (2011) are in posterior views); see Table 6 from Sekiya (2011) for measurements, the values from ulnar and radial distal width of holotype (*Chuanjiesaurus anaensis* need be exchanged). Length of radius is 0.64 length of humerus. Proximally, the maximum width is 24% of the total length (*Chuanjiesaurus anaensis* is 21%). Proximal end is nearly oval with a mildly concave medial surface that met the anteromedial process of ulna. The oval shape of that is similar to early diverging sauropods (e.g. *Vulcanodon karibaensis, Shunosaurus lii*), some mamenchisaurids, *Barapasaurus tagorei*, and *Camarasaurus lewisi* (Cooper 1984; Dong et al. 1983; He et al. 1996; Tang et al. 2001; Bandyopadhyay et al. 2010; McIntosh et al. 1996). The surface of the proximal end is nearly flat with a slightly concave area in the centre, and there is a bump anteromedially, this condition is also present in *Chuanjiesaurus anaensis, Omeisaurus tianfuensis, Patagosaurus fariasi, Camarasaurus lewisi*, and *Saltasaurus loricatus* (Bonaparte 1986; Powell 1992; McIntosh et al. 1996; He et al. 1998; Fang et al. 2000). The surface of the proximal end is nearly perpendicular to the axis of the shaft. This condition is similar to *Omeisaurus tianfuensis, Patagosaurus fariasi*, and *Camarasaurus lewisi* (Bonaparte 1986; McIntosh et al. 1996; He et al. 1998). The cross section of radial mid-shaft is elliptical.

The distal surface of the radius is flat, with an elliptical shape. A prominent elongated convex area exists on the posteromedial surface of distal portion (Figure 6, pmcr). The distal radial condyle is flat and respects to the long axis of shaft are nearly perpendicular, which is similar to most of sauropods (e.g. *Vulcanodon karibaensis, Shunosaurus lii*, mamenchisaurids, and *Apatosaurus ajax*).

Metacarpals

There are five metacarpals of the left side preserved *in-situ* (Figure 2; Figs. 44–48 (Sekiya (2011)), the proximal surface of each metacarpal is downwards, and the distal surface of each metacarpal is upwards; see Table 7 from Sekiya (2011) for measurements). The ventral surfaces are still buried and invisible. The first, fourth and fifth metacarpals are complete, whereas the second metacarpal lacks the distal end and the third one is represented by the proximal half only.

Metacarpal I is a robust and short element. The total length of metacarpal I is 0.3 the length of radius. This element is approximately quadrangular in outline when viewed in dorsal aspect, being shorter lateromedially than proximodistally. The dorsal surface of the proximal end is slightly dorsomedially inclined. It is gently twisted about the long axis such that the medial condylar area wraps laterally, in addition to arching dorsally at both the proximal and distal extremities. The Mc-I has a sub-triangular shape in proximal view, similar to that in *Shunosaurus lii* and *Barapasaurus tagorei* (proximally, the most dorsally extended margin situated on the middle portion of dorsal margin, consists the apex of the isosceles triangle in outline in the two taxa. By contrast, the apex on the lateral portion of dorsal margin, makes an oblique triangle in outline in *Analong*), whereas *Omeisaurus tianfuensis* share a more sharp triangle pointing and rounded dorsal surface.

The edge of proximal surface is slightly declined and is roughly trapezoidal in shape with longer ventroproximal end compared with the dorsoproximal end. The dorsomedial edge of proximal surface is

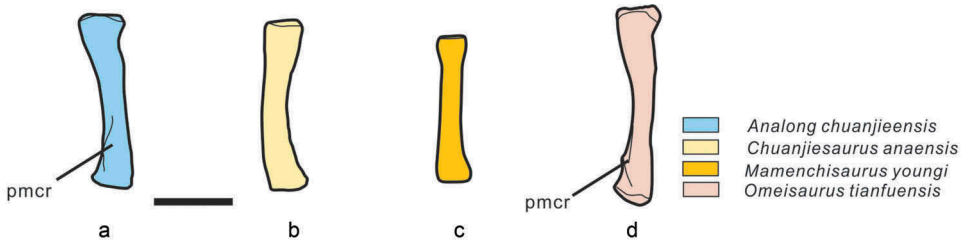

Figure 6. Comparison of radius of *Analong chuanjieensis* (A), *Chuanjiesaurus anaensis* (B), *Mamenchisaurus youngi* (C) and *Omeisaurus tianfuensis* (D) in posterior views. (A, B and D) Left radius. (C) Right radius. Scale bar equals 30 cm. Abbreviation: pmcr, posteromedial convex of lower part of radius.

also declined, whereas it could be caused by poor preservation. The dorsolateral margin of the proximal end lacks the rounded bulges that characterise metacarpal I instead, there is a notch on the middle portion of dorsolateral margin. This character also exists in *Shunosaurus lii, Barapasaurus tagorei* and *Omeisaurus tianfuensis* (more prominent) (Zhang 1988; He et al. 1998; Bandyopadhyay et al. 2010). On the dorsal surface, a small shallow fossa in housed in the space near the distal end. Between the proximal and distal articular faces, the lateral surface is gently narrower than its medial counterpart except the preservation factors and the lateral surface is slightly concave to contacts with metacarpal II. The metacarpals are slightly twisted along its axis, so that the proximal half of the dorsal surface faces dorsomedially, whereas the distal half faces dorsally. This condition also exists in *Omeisaurus tianfuensis*, contrasts with the condition in *Shunosaurus lii, Barapasaurus tagorei* and titanosauriforms, whereby the distal end is perpendicular to the long axis of the shaft (He et al. 1998; Zhang 1988; Bandyopadhyay et al. 2010; Mannion et al. 2019). Distally, the lateral condyle is inclined to face distolaterally and is more expand than the medial counterpart, expanding laterally in an extension that also flares laterally. The articular surface is elliptical and flat with gently concave centre. The dorsal surface is flat, compare with other round surface in distal view.

The remaining metacarpal II is a slender and rod-like element with the proximal and middle part preserved. It is discernibly shorter than Mc-I, are sub-equal in overall form and length. The proximal width is 0.07 the length of radius, which is the lowest value among mamenchisaurids (others about 0.13). Mc-II is the most slender element among the five metacarpals. Mc-II is quadrangle-like in proximal view and the proximal face is convex in dorsal aspect, whereas that in *Omeisaurus tianfuensis* is trapezoid with shorter dorsal surface than the ventral surface. Both lateral and medial surfaces are parallel to each other respectively, whereas both of the medial and lateral surfaces of proximal end are concave in *Omeisaurus tianfuensis* (He et al. 1998). The middle section is gently expanded in all directions (expect the ventral surface for the buried reason) more so than the proximal surface. Both of the proximal and distal regions of the medial surface have shallow fossa, and the medial surface of middle portion is shallower than its counterpart. By contrast, the lateral surface of Mc-II is convex with smooth ridges dorsally and ventrally. The distal end is not complete, and the cross section of preserved portion is elliptical shaped.

The metacarpal III is robust and also preserved in proximal view. Based on the preserved portion, the shaft of this element gently twisted about the long axis such that the proximolateral area twisted medially. The proximal width is 0.15 the length of radius. The proximal end is slightly convex and with an elliptical shape in proximal view, whereas that in *Omeisaurus tianfuensis, Shunosaurus lii* and many other basal taxa such as *Barapasaurus tagorei* share a trigonal proximal end (Zhang 1988; He et al. 1998; Bandyopadhyay et al. 2010). The dorsal surface of the proximal end is slightly convex, similar to that in *Shunosaurus lii* and *Barapasaurus tagorei* (Zhang 1988; Bandyopadhyay et al. 2010), whereas that in *Omeisaurus tianfuensis* is flat (He et al. 1998). The medial and lateral surfaces are convex, and the dorsal surface is concave with a convex proximal end. In dorsal view, the shaft curved medially.

The metacarpal IV has a straight shaft in its distal half than the proximal counterpart. Mc-IV is the longest element among all preserved metacarpals, the total length of the shaft is 0.38 the length of radius. The shape of proximal end is triangle, which is generally similar to *Barapasaurus tagorei*, whereas the shape of *Omeisaurus tianfuensis* is oval (He et al. 1998; Bandyopadhyay et al. 2010). By contrast, the proximal end with a slightly concave medial surface in *Analong chuanjieensis*, proximal end with concave on dorsal surface in *Omeisaurus tianfuensis*, and no prominent concave on medial, lateral and dorsal surfaces of proximal end in *Barapasaurus tagorei* (He et al. 1998; Bandyopadhyay et al. 2010). Both of proximal and distal ends culminate in moderately expanded articular surfaces. In contrast, the proximal half of Mc-IV is curved and flared medially. More so, the proximal end is expanded mediolaterally, than the shaft itself. The medioproximal half of proximal end is more expand than the lateroproximal half. The proximal surface is mildly medioproxiomally oriented. In dorsal view, the proximal surface is about 79 degrees to the shaft, and the distal surface is perpendicular to the shaft. Regarding the proximal surface, the ventral margin is slightly higher than the dorsal edge. The medial portion of proximal surface is slightly convex share a faintly apical. The medioproximal half of the proximal surface is especially narrow, but expands moderately lateroproximally, resulting in a wedge-shaped proximal articular surface. The proximal half of the dorsal surface is prominently depressed compare with the distal half. The medial and lateral margins are concave for the expanded proximal and distal ends in dorsal view, but overall both of the medial and lateral surfaces are flat. The distal surface is generally flat with mildly concave on the middle portion. The medial condyle is elliptic-shaped, and the lateral condyle is quadrilateral-shaped in distal view. The intercondylar groove is well developed on the medial part of the distal surface.

The metacarpal V is a robust bone with a straight shaft in its proximal half than the distal counterpart. Most of the element is well persevered except the dorsolateral corner of proximal end. The total length of the shaft is 0.31 the length of radius. Both of proximal and distal ends culminate in moderately expanded articular surfaces, and the distal end is slightly more expand than the proximal one. The medial and lateral parts of the proximal articular surface are flat. The dorsal surface of the proximal articular is slightly concave in the central part in proximal view, whereas that in *Omeisaurus tianfuensis* is convex. The ventral surface of the proximal articular is invisible for it is still be buried as is the distal articular end. The distal half of Mc-V is curved and flared laterally. The proximal end expands more mediolaterally than the shaft itself. The lateroproximal half of proximal end is more expand than the medioproximal half. In dorsal view, the proximal surface is perpendicular to the shaft, and the distal surface is about 60 degrees to the shaft. Regarding the proximal surface, the middle portion is slightly higher than the dorsal and ventral edges. The dorsal portion of proximal surface is prominently concave. Both of medioproximal and lateroproximal ends of proximal surface is flat in proximal view. The medial surface is flat, and the lateral surface is concave for the expanded lateroproximal and laterodistal ends in dorsal view. The dorsal surface faintly concave and this concave proximodistally extend. The lateral surface of the shaft is concave, makes the shaft looks a little curve. In distal view, the medial and the lateral surfaces are flat, and the dorsal surface is concave slightly. The distal surface is generally flat with slightly concave middle portion. The lateral condyle is more robust than the medial one, and the distal surface is wedge-shape in distal view. The intercondylar groove is on the medial part of the distal surface and well developed.

Ilium

A complete left ilium is preserved and partly articulated to the sacral vertebrae (Figures 2 and 5; Fig. 49 (Sekiya (2011)); see Table 8 from Sekiya (2011) for measurements). The ilium has a strongly convex dorsal margin in lateral view. It is similar in overall morphology to that of other sauropods, such as mamenchisaurids and other advanced sauropods. The highest point on the dorsal margin of the ilium lies

posterior to the base of the pubic peduncle, similar to that in *Shunosaurus lii, Barapasaurus tagorei, Camarasaurus lewisi*, and *Apatosaurus ajax* (Zhang 1988, Fig. 51; Bandyopadhyay et al. 2010, Fig. 11; McIntosh et al. 1996, Fig. 67; Upchurch et al. 2004, Fig. 9). The pre-acetabular process is sub-triangular and projects anterolaterally. In lateral view, the pre-acetabular process projects beyond the anterior end of the pubic peduncle, resembling that in *Omeisaurus tianfuensis*, and *Mamenchisaurus youngi*. The angle between the ventral margin of the pre-acetabular process and the anterior margin of the pubic peduncle is close to 90 degrees, similar to *Shunosaurus lii, Apatosaurus ajax* and *Omeisaurus tianfuensis*, whereas this angle is little more acute in *Mamenchisaurus youngi*. The pre-acetabular process increases in thickness ventrally. The dorsal surface of the ilium, including the pre-acetabular and postacetabular processes, shares a wrinkled texture. The postacetabular process extends posterolaterally with a sub-square shaped distal end, contrasting with the pointed postacetabular process of a number of sauropods. This shape of distal end is not natural and it may be deformed during preservation. The position of the ischial peduncle is higher than the distal part of the ilium plane with the ischial peduncle and pubic peduncle on the same plane in lateral view. Except for the early branching sauropods such as *Shunosaurus lii*, almost all advanced taxa share this character. In lateral view, the postacetabular exhibits a flat ventral margin, similar to that in *Cetiosaurus oxoniensis, Patagosaurus fariasi*, whereas in other taxa such as *Mamenchisaurus youngi, Saltasaurus loricatus, Amargasaurus cazaui* possess an almost slightly convex ventral margin (Figure 5, vb). The distal end of the ischiac peduncle of the ilium is flat without a heel.

The pubic peduncle projects ventrally and a little anteriorly. It extends below the main body of the ilium approximately, and it expands transversely. In horizontal cross-section, the posterior surface of pubic peduncle is deeply concave. The anterior, posterior, lateral and medial surfaces merge smoothly into each other. Consequently, the distal end surface is also sub-rectangle in outline with slightly anteroposteriorly compressed middle portion. The ischiac peduncle is greatly reduced dorsoventrally, resembling that in advanced sauropods. Moreover, a straight line extending through the articular surfaces of the pubic and ischiac peduncles passes just beneath the ventral margin of the postacetabular. Additionally, the ventrolateral surface of the postacetabular lacks a distinct brevis fossa, resembling that in all sauropods (Gauthier 1986).

Pubis

Both pubes are well preserved (Figure 2; Fig. 50 (Sekiya (2011)); see Table 9 from Sekiya (2011) for measurements). The left pubis appears to be somewhat longer and more robust than the right one, possibly due to taphonomic distortion. In proximal view, the pubis bears a shallowly articular surface, transversely expanded with wrinkled articulation for the pubic process of the ilium. Still, the peripheral rim of iliac articulation develops smoothly anteroposteriorly. The length of iliac articular surface is 0.28 proximodistal length of pubis. The ambiens process is not prominent below the anterior tip of the iliac articulation.

The acetabular articular surfaces are slightly expanding transversely and concave in lateral view, and it decreases in transverse width to the margin of ischiac articulation. The ischiac articulation is also slightly expanding mediolaterally and contain a small concave on the middle portion of the surface. The length of ischiac articular surface is 0.31 the total length of pubis. This is the plesiomorphic state typical of most sauropods and contrasts with the relatively longer articular surface exist in advanced taxa such as macronarians (Salgado et al. 1997; Upchurch et al. 2004). The obturator foramen is invisible because it is obscured by surrounding rocks covering. The two pubes are in articulation from the posterior end of the ischiac articular to the middle portion of the total length. The length of the articulation is about 0.32 the total length of pubes.

In horizontal cross-section, the pubic shaft has a 'comma'-shape, which is similar to that in other sauropods. This is formed by a shallowly concave medial surface, a flat lateral surface, and an acute flange-like posterior margin. As the shaft approaches the distal end, the anterior and the posterior portions of the distal end generally expand anteroposteriorly. The anterior portion of the distal end is much more robust than the posterior portion. The posterodistal end of left pubis is much acute, whereas that on the right pubis is much smooth, according to the preservation of surfaces the posterodistal portion of right pubis maybe lost the end part of the posterodistal portion. The distal width is approximately 40% of the total length of the pubis according to the present preservation (the left: about 43% [estimated; preserved value: 33%]; the right: about 40%), the actual ratio could be even bigger considering the lost part of posterodistal portion of right pubis. This value is the greatest among mamenchisaurids (other taxa of mamenchisaurids are below 30%).

Femur

The femur is well preserved with the anterior surface exposed (Figure 2; Fig. 53 (Sekiya (2011)); see Table 11 from Sekiya (2011) for measurements). Lesser trochanter is absent, similar to that in eusauropods such as *Omeisaurus tianfuensis, Camarasaurus lewisi, Saltasaurus loricatus*. The head projects mainly medially and slightly dorsally, which has been reported in other sauropods such as *Omeisaurus tianfuensis, Mamenchisaurus youngi, Barapasaurus tagorei, Patagosaurus fariasi* and *Jobaria tiguidensis*, but does not resembles the condition in some sauropods such as *Chuanjiesaurus anaensis, Shunosaurus lii* and *Chubutisaurus insignis*, with more dorsally directed head. Lateral bulge (refer to Salgado et al. 1997), defined as marked by the lateral expansion and a dorsomedial orientation of the dorsolateral margin of the femur, is weak (Figure 7, lb), similar to that in *Tazoudasaurus naimi, Barapasaurus tagorei, Patagosaurus fariasi, Mamenchisaurus youngi*, and some derived taxa such as *Brachiosaurus*, but this feature prominently exists in *Chuanjiesaurus anaensis*, and some derived taxa such as *Saltasaurus loricatus*. Distal articular surface is restricted to distal portion of femur, similar to that in most sauropods such as *Chuanjiesaurus anaensis* and *O. tianfuensis*.

Phylogenetic analysis

A phylogenetic analysis was conducted to assess the affinities of *Analong chuanjieensis* within Sauropoda (Figure 8). A maximum parsimony analysis is performed based on the data set of Xu et al. (2018), with 375 original characters plus 11 new characters by this study (see the Supplementary Data). We revised seven scoring errors in the previous matrix (*Omeisaurus tianfuensis*: 2 to 1 (Ch. 181) and 0 to 1 (Ch. 198); *Mamenchisaurus youngi*: 1 to 0 (Ch. 126) and 0 to 1 (Ch. 198); *Chuanjiesaurus anaensis, Analong chuanjieensis* and *Yuanmousaurus jiangyiensis*: 0 to 1 (Ch. 198)). Coding of these new characters are based on extensive review of the literatures (e.g. Upchurch 1998; Wilson and Sereno 1998; Wilson and Upchurch 2003; Sekiya 2011; Mannion et al. 2013; Huang et al. 2014; Poropat et al. 2016; Ren et al. 2018), as well as our personal observations. Some characters were treated as ordered (as in Xu et al. 2018). See supplement material for the complete character list and MESQUITE version of the data matrix. The matrix was subjected to in TNT v. 1.5 (Goloboff and Catalano 2016), see method part for details.

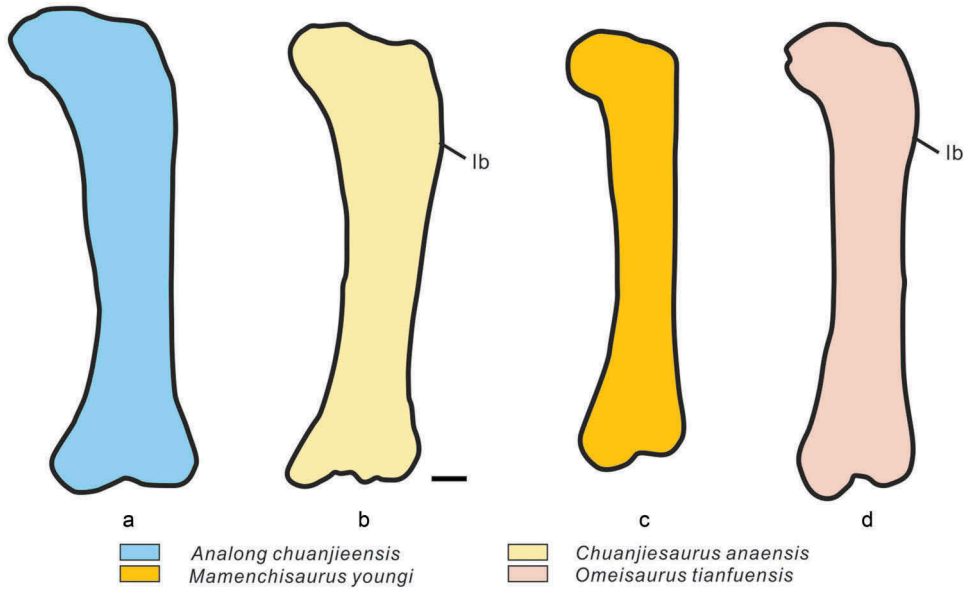

Figure 7. Comparison of femur of *Analong chuanjieensis* (A), *Mamenchisaurus youngi* (C), *Chuanjiesaurus anaensis* (B), and *Omeisaurus tianfuensis* (D) in anterior views. (A and C) Left femur. (B and D) Right (Left in reverse) femur. Scale bar equals 10 cm. Abbreviation: lb, lateral bulge.

A strict consensus of all 18 most parsimonious trees (tree length = 1217 steps; consistency index = 0.375; retention index = 0.703) supports a monophyletic Mamenchisauridae. *Analong chuanjieensis* is recovered as the earliest diverging branch of this Mamenchisauridae clade, followed by *Omeisaurus tianfuensis, Yuanmousaurus jiangyiensis, Mamenchisaurus youngi*, and *Chuanjiesaurus anaensis* successively.

The mamenchisaurid clade is supported by eight unambiguous synapomorphies ('0' to '1' for character 152, 198, 376; '0' or '1' to '3' for character 115; '0' to '2' for character 174; '1' to '0' for character 125, 305 and 377), including a character that mamenchisaurid share with other sauropod (e.g. Turisauria also share this character). *Analong chuanjieensis* share all these eight characters ('pleurocoels with division (character 115)'; 'height of the neural arch less than the height of the posterior articular surface of middle cervical vertebrae (character 125)'; 'hyposphene-hypantrum system is present but weakly developed on the posterior dorsal vertebrae (character 152)'; 'articular face shape of posterior dorsal centra are opisthocoelous or slightly opisthocoelous (character 174)'; 'anterior caudal transverse processes with "wing-like" shape (character 198)'; 'transverse breadth of distal condyles of femur are sub-equal (character 305)'; 'two accessary processes on the anterodistal end of humerus (character 376)'; 'medial accessory process is more robust than the lateral one between the two humeral accessary processes (character 377)'). *Omeisaurus tianfuensis* and other clade within Mamenchisauridae is supported by three synapomorphies ('0' to '1' for character 124, 126 and 386): Lateral fossae on the prezygapophysis process on middle cervical vertebrae are present (character 124); Middle cervical centrum, anteroposterior length divided the height of the posterior articular surface is more than four (character 126); Length of dorsal surface of proximal end of Mc I is equal to or longer than ventral surface (character 386). *Yuanmousaurus jiangyiensis* and other mamenchisaurids clade is supported by three synapomorphies ('Anterior and middle dorsal vertebrae, zygapophyseal articulation angle posteroventrally oriented (character 149)'; 'Middle and posterior dorsal neural arches, posterior centroparapophyseal lamina (PCPL) is absent (character 161)'; 'Tibial proximal condyle, shape is narrow, long axis expanded transversely, condyle sub-circular (character 309)'). The (*Mamenchisaurus youngi* + *Chuanjiesaurus anaensis*) clade is supported by four synapomorphies ('0' to '1' for character 237 and 305; '0' to '2' for character 379; '1' to '0' for character 385): Scapula, ventral margin with a well developing ventromedial process (character 237); Transverse breadth of distal condyles of femur are sub-equal (character 305); Anterior caudal centra, anteroposterior length of posterior condylar ball to mean average radius ([mediolateral width + dorsoventral height] divided by 4) of anterior articular surface of centrum ratio is greater than 0.3 (character 379); Anterodorsal margin of anterior caudal neural spines level with or posterior to posterior margin of postzygapophyses (character 385).

Discussion

Though preserved in the same quarry, comparative morphology suggests that *Chuanjiesaurus anaensis* (Fang et al. 2000) is different from *Analong chuanjieensis*. Firstly, caudal transverse processes of *Analong chuanjieensis* persist until the 10th caudal, while, that in *Chuanjiesaurus anaensis* they persist until the 15th caudal. Secondly, the ratio of dorsoventral length of anterior caudal centrum to anteroposterior length of anterior caudal centrum (without ball) in *Chuanjiesaurus anaensis* is bigger than that in *Analong chuanjieensis* (e.g. height of posterior surface/length of centrum on Cd 9 in *Chuanjiesaurus anaensis* is 1.4, and that in *Analong chuanjieensis* is 1.1; see Lc/Hca and Lc/Hcp on Tables 3–4 from Sekiya (2011)) (Figure 9A). It indicates that the centrum in *Analong chuanjieensis* is more prominent in anteroposterior extent than *Chuanjiesaurus anaensis*. Additionally, in the anterior caudal centra of *Analong chuanjieensis*, the ratio of the anteroposterior length of posterior condylar ball to the mean radius of anterior articular surface (aBR) is about 0.27, by contrast, that in *Chuanjiesaurus anaensis* is about 0.44. It indicates that the posterior condylar surfaces of *Chuanjiesaurus anaensis* are more convex than that in *Analong chuanjieensis*. Additionally, the ratio of the height of the caudal neural arch to the length of caudal centra in *Chuanjiesaurus anaensis* is prominently greater than that in *Analong chuanjieensis*

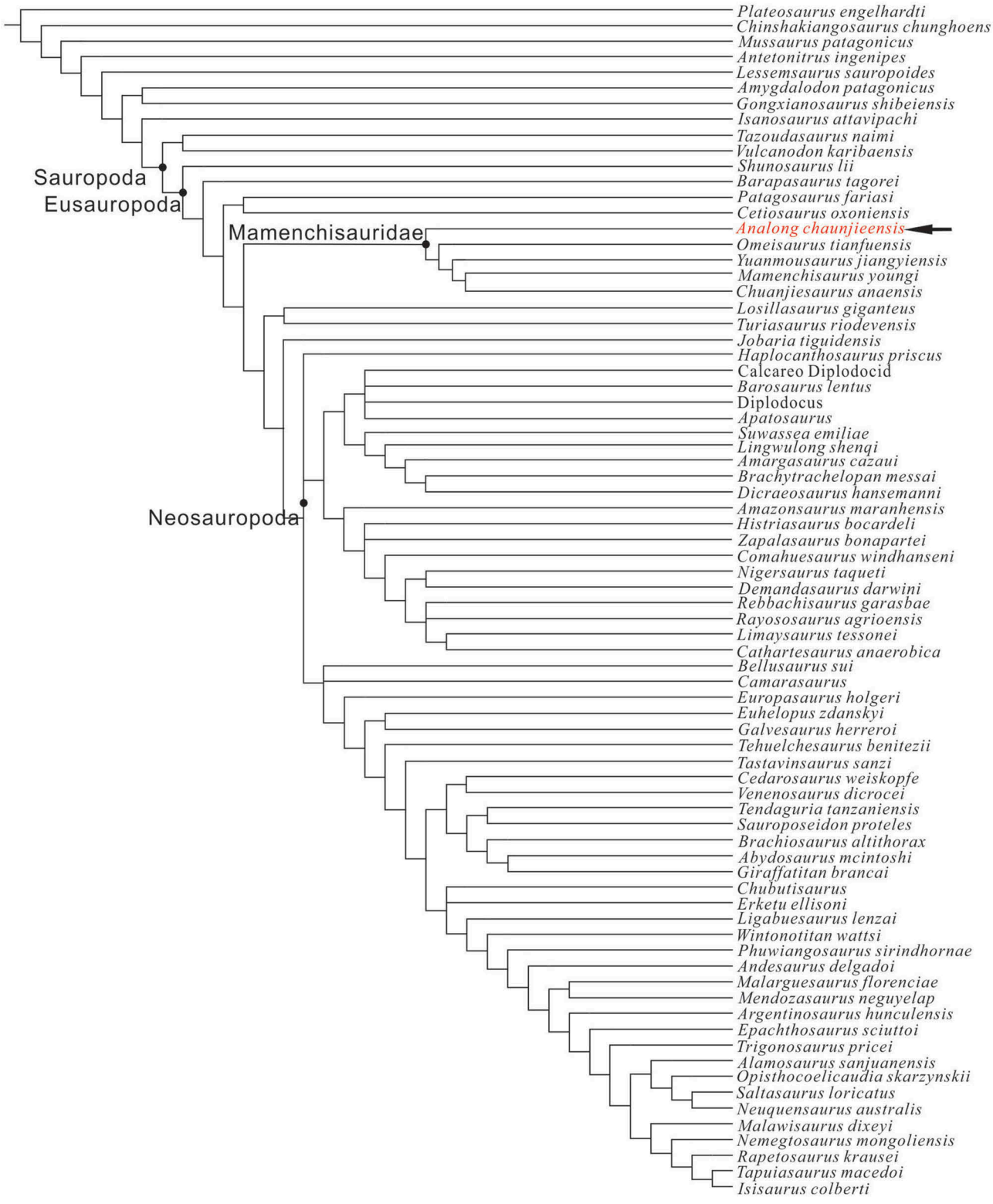

Figure 8. Strict consensus of 18 MPTs (TL = 1217 steps) from phylogenetic analysis (76 taxa, 386 characters). The data matrix follows Xu et al. (2018), with the addition of 11 character codings for *Analong chuanjieensis* (see Appendix 1).

(Figure 9B). Thirdly, the ratio of the length of neural spines of anterior caudal vertebrae to the height of centra in *Analong chuanjieensis* are below 1.0 (about 0.9), while the value are greater in *Chuanjiesaurus anaensis* (about 1.2 to 1.4). The ratio of the length of caudal neural spine to the length of caudal centrum in *Chuanjiesaurus anaensis* is also distinctly greater than *Analong chuanjieensis* (Figure 9C). Beyond that, the SPRL and SPOL are prominent from the base to the summit of neural spine along the anterolateral margin on the anterior caudals, and the two types of lamina slightly anterolaterally and posterolaterally oriented, respectively, in *Chuanjiesaurus anaensis*, which makes a concavity on the lateral side of the neural spine. By contrast, the SPRL and SPOL are

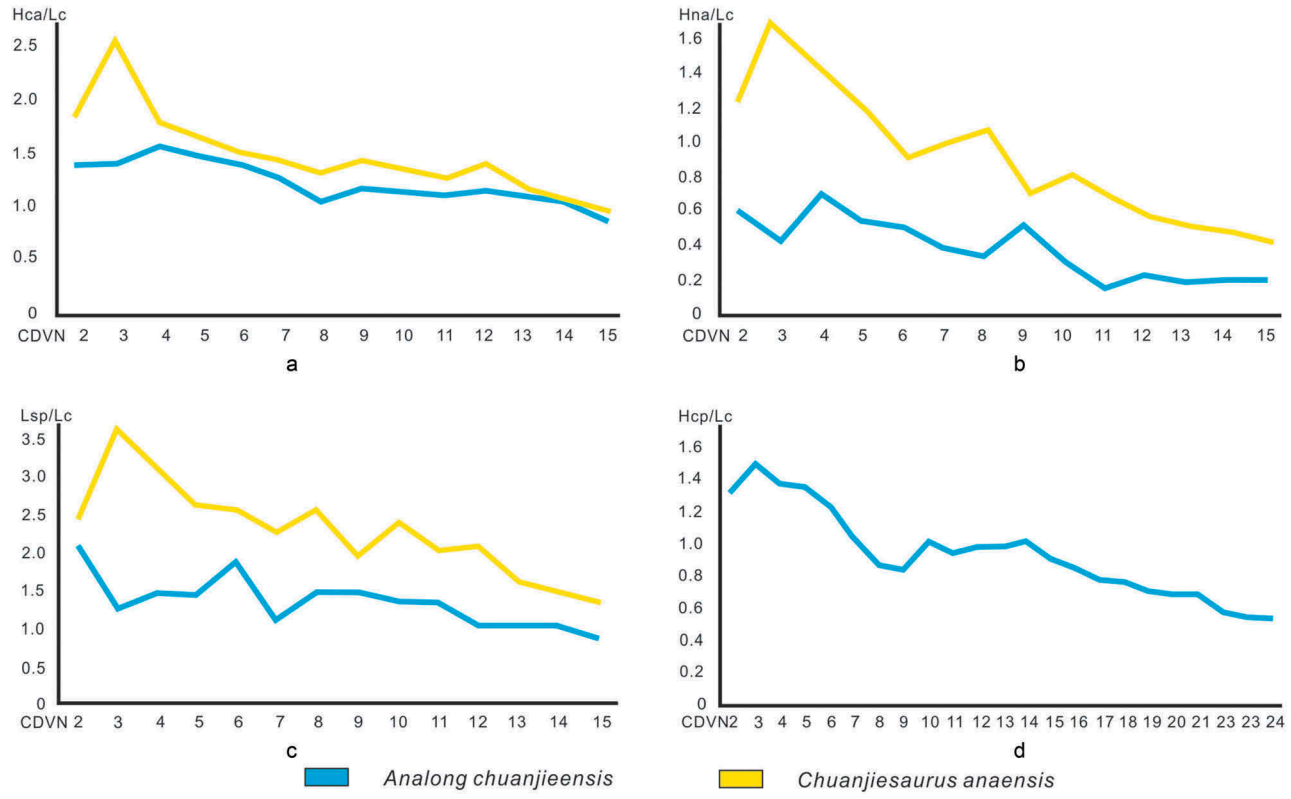

Figure 9. Some caudal ratios of *Analong chuanjieensis* and *Chuanjiesaurus anaensis*. (A, B and C), Hca/Lc, Hna/Lc and Lsp/Lc of anterior caudals between *Analong chuanjieensis* and *Chuanjiesaurus anaensis*. (D), Hcp/Lc of caudals of *Analong chuanjieensis*. All ratios are calculated by measurements (Sekiya (2011)) and conjectural values. Abbreviations: hca, height of anterior surface of the centrum; hcp, height of posterior surface of the centrum; hna, height of neural arch; lc, length of centrum; lsp, length of neural spine; cdvn, caudal vertebra number.

small short ridges that rapidly fade out into the anterolateral margin of the spine on anterior caudals, and the lateral surface of anterior caudal neural spines are slightly convex in *Analong chuanjieensis*. Fourthly, the shape of the humeral proximolateral corner of *Analong chuanjieensis* is rounded, while that in *Chuanjiesaurus anaensis* is square. Additionally, the medial portion of humeral proximal end is more expanded than the lateral portion in *Chuanjiesaurus anaensis*, whereas the two portions are almost equally expanded in *Analong chuanjieensis*. Moreover, the middle part of humeral proximal end of *Analong chuanjieensis* is much broader than that in *Chuanjiesaurus anaensis*. Fifthly, compared with the medial condyle, the lateral condyle of humerus in *Analong chuanjieensis* is much greater than that in *Chuanjiesaurus anaensis*. Sixthly, the relative length of the two ulnar proximal condylar processes of *Analong chuanjieensis* is subequal, while that in *Chuanjiesaurus anaensis* is unequal. Also, the angle between the two processes of *Analong chuanjieensis* is about 45 degrees, by contrast, that in *Chuanjiesaurus anaensis* is 60 degrees. Additionally, a distinct proximodistally extended concavity on the medial surface of left ulna of *Analong chuanjieensis*, whereas that concave does not exist in *Chuanjiesaurus anaensis*. Seventhly, the cross section of the ulnar mid-shaft differs between the two taxa, with *Analong chuanjieensis* bearing a circular shape compared with an elliptical one of *Chuanjiesaurus anaensis*. The distal shape of ulna is sub-quadrangle in *Chuanjiesaurus anaensis*, whereas it is elongated and oval in *Analong*. Eighthly, the radius of *Chuanjiesaurus anaensis* has a straight shaft in its proximal half than the distal counterpart with the distal half strongly medially extend, whereas the radius of *Analong chuanjieensis* has a straight shaft in its distal half than the proximal counterpart. The orientation of distal surface is slightly mediodistal in *Chuanjiesaurus anaensis*, by contrast, it is laterodistal in *Analong chuanjieensis*. A protuberance exists on the medial part of proximal end and is medioposteriorly oriented in *Analong chuanjieensis*, this character in *Chuanjiesaurus anaensis* is absent. The distal surface shares a concavity on the posterior margin. Additionally, PMCR exists on the lower part of posteromedial surface of radius in *Analong chuanjieensis*, whereas it is absent in *Chuanjiesaurus anaensis* with a generally smooth posteromedial surface. Ninthly, the femoral head of *Analong chuanjieensis* projects mainly medially, while that in *Chuanjiesaurus anaensis* projects dorsally. Moreover, the lateral bulge is absent in *Analong chuanjieensis*, while it exists in *Chuanjiesaurus anaensis*.

The morphological comparison also suggests that *Omeisaurus tianfuensis* (He et al. 1998) is different from *Analong chuanjieensis*. First of all, the pneumatization of cervical centra is much simpler in *Analong chuanjieensis* than that in *Omeisaurus tianfuensis*. Pneumatic fossae in cervical centra of *Analong chuanjieensis* are divided into several shallow fossae, whereas that in *Omeisaurus tianfuensis* are more complex. For example, some pneumatic fossae in *Omeisaurus tianfuensis* are extremely deep, to the extent that in some cervicals both sides could be interconnected with a penetrated hole in lateral view. Some pneumatic fossae are divided by several laminae in the deep position, creating many secondary fossae in *Omeisaurus tianfuensis*. Additionally, in the middle cervical centra, the ratio of the anteroposterior length divided by the height of the posterior articular surface in *Analong chuanjieensis* is below 4.0 (about 3.8), while that in *Omeisaurus tianfuensis* are more than 4.0. This results in makes *O. tianfuensis* having a more elongated neck than *Analong chuanjieensis*. Next, *Analong chuanjieensis* possesses procoelous anterior caudal centra, while anterior caudal vertebrate are amphiplatyan in *Omeisaurus tianfuensis*.

Additionally, it also means that *Analong chuanjieensis* is the basal most taxon with procoelous anterior caudal vertebrae among the Mamenchisauridae clade according to the phylogenetic analysis. Although both *Chuanjiesaurus anaensis* and *Mamenchisaurus youngi* share procoelous articular faces, the value of aBR in *Analong chuanjieensis* is lowest among them. Besides, caudal transverse processes persisting until the 15th caudal in *Omeisaurus tianfuensis*, and that in *Analong chuanjieensis* is the 10th caudal. Thirdly, the ulna of *Omeisaurus tianfuensis* is more slender than that in *Analong chuanjieensis* according to the cross section of each shaft of the two taxa. The angle between the ulnar anterolateral process and the anteromedial process of *Omeisaurus tianfuensis* is 85 degrees, whereas the angle is 45 degrees in *Analong chuanjieensis*. Additionally, the femoral laterally bulge is pronounced in *Omeisaurus tianfuensis*, while it is absent in *Analong chuanjieensis*.

Wamweracaudia keranjei was reported as a new mamenchisaurid from Tanzania (Mannion et al. 2019). A sequence of 30 caudal vertebrae is articulated in the holotype of *Wamweracaudia keranjei*. The morphological analysis suggests that this taxon is different from *Analong chuanjieensis*. Firstly, the posterior articular faces of anterior caudal centra of *Wamweracaudia keranjei* are strongly expanded, whereas that in *Analong chuanjieensis* are less expanded (aBR value: *Analong chuanjieensis*, lower than 4.0; *Wamweracaudia keranjei*, more than 4.0). Secondly, two prominent ventrolateral ridges occur on the ventrolateral surface of middle caudal vertebrae in *Analong chuanjieensis*, while *Wamweracaudia keranjei* does not share this character. Thirdly, though *Wamweracaudia keranjei, Analong chuanjieensis*, and *Chuanjiesaurus anaensis* share a 'wing-like' transverse process, it curves anteriorly in the *Wamweracaudia keranjei*, whereas in *Analong* and *Chuanjiesaurus* it is laterally oriented. Fourthly, a prominent lateral tubercle (ltu) is situated on the dorsal surface of transverse processes of anterior caudal vertebrae in *Wamweracaudia keranjei*, which is absent in *Analong chuanjieensis* and *Chuanjiesaurus anaensis*. Moreover, there is also an upper tubercle on the medial side of ltu in *Wamweracaudia keranjei*, whereas *Analong chuanjieensis* and *Chuanjieensis anaensis* do not share this character. Fifthly, the ACDLs are also on the ventral surface of transverse process of anterior caudal vertebrae in *Wamweracaudia keranjei*, whereas this character is absent in *Analong chuanjieensis* and *Chuanjiesaurus anaensis*. Sixthly, the SPOLs exist in *Wamweracaudia keranjei*, while no distinct laminae connect postzygapophyses to neural spines in *Analong chuanjieensis* and *Chuanjiesaurus anaensis*.

Analong chuanjieensis also possesses some autapomorphies such as caudal transverse processes only persisting until the 10th caudal. The number of caudal vertebrae with transverse processes in other taxa of Mamenchisauridae is 15. The articular surfaces of the anterior caudal centra are procoelous; the anteroposterior length of the posterior condylar ball divided by the mean radius of anterior articular surface of centrum is about 0.27, which is the lowest value among mamenchisaurids. Bifid chevrons exist in middle series. Moreover, length of ulnar proximal condylar processes are sub-equal, and the angle between the ulnar anterolateral process and anteromedial process is about 45 degrees. It is also the lowest value among mamenchisaurids. Proximal width of metacarpal II 7% the length of radius, which is the lowest value among mamenchisaurids. Additionally, distal width approximately 40% the total length of the pubis (the greatest value among mamenchisaurids).

Chuanjiesaurus can be diagnosed by the following unique combination of revised character states (autapomorphies marked with an *): caudal transverse processes persisting until the 15th caudal. Anteroposterior length of posterior condylar ball to mean average radius of anterior articular surface of centrum ratio (aBR) is about 0.44*. The length of neural spines/the height of centra in anterior caudal vertebrae are about 1.2–1.4*. Dorsoventral height of scapular acromion process to minimum dorsoventral height of scapular blade ratio is 3.0. Total length of humerus is 0.77 length of femur, total length of ulna is 0.68 length of humerus, and total length of radius is 0.62 length of humerus.

Conclusion

At least two mamenchisaurid sauropod genera exist in the quarry of the Lufeng World Dinosaur Valley. The new genus *Analong chuanjieensis* represents the earliest branching of Mamenchisauridae while *Chuanjiesaurus anaensis* is a latter diverging taxon among mamenchisaurids and is more closely related to *Mamenchisaurus youngi*.

Analong chuanjieensis enriches the diversity of early branching sauropods and provides additional information to help understand the evolutionary history of sauropods in southwest China. The basal and diverged mamenchisaurid taxa living in same area and period indicates that Mamenchisauridae is a more complicated scenario in the evolution of sauropod.

Abbreviation

Institutional abbreviations

FRCC Fossil Research Center of Chuxiong Prefecture, Yunnan, China

LCD Word Dinosaur Valley, Chuanjie Town, Lufeng County, Yunnan, China

LFGT Bureau of Land and Resources of Lufeng County, Yunnan, China

UARK University of Arkansas, Fayetteville, Arkansas, USA

Anatomical abbreviations

abr, anteroposterior length of posterior condylar ball to the mean radius of anterior articular surface; ca, cervical vertebra; cd, caudal vertebra; cdf, centrodiapophyseal fossa; cdvn, caudal vertebra number; clp, anterolateral process; cmp, anteromedial process; cpas, cervical posterior accessory septum; cpol, centropostzygapophyseal lamina; cprl, centroprezygapophyseal lamina; cprl-f, centroperzygapophyseal lamina fossa; dn, dorsal vertebrae number; dpc, deltopectoral crest; hca, height of anterior surface of the centrum; hcp, height of posterior surface of the centrum; hna, height of neural arch; hri, the average of the greatest widths of the proximal end, mid-shaft and distal end of humerus/length of humerus; lap, lateral accessory process; lb, little bulge; lc, length of centrum; lp, lateral process; lsp, length of neural spine; map, medial accessary process; mep, medial part of proximal surface; mc, metacarpal; mip, middle part of proximal surface; pcdl, posterior centrodiapophyseal lamina; pcpl, posterior centroparapophyseal lamina; pf, lateral pneumatic fossa or foramen; plp, proximolateral process; pmcr, posteromedial convex of lower part of radius; podl, postzygodiapophyseal lamina; pocdf, postzygapophyseal centrodiapophyseal fossa; prcdf, prezygapophyseal centrodiapophyseal fossa; ppdl, paradiapophyseal lamina; prdl, prezygadiapophyseal lamina; prpl, prezygoparapophyseal lamina; spdl, spinodiapophyseal lamina; spol, spinoprezygapophyseal lamina; sprl, spinoprezygapophyseal lamina; tpol, intrapostzygapophyseal lamina; tprl, intraprezygapophyseal lamina; urp, angle between anterolateral and anteromedial processes of ulna; url, ratio of length of anterolateral process to total length of ulna; urm, ratio of length of anteromedial process to total length of ulna; vb, ventral bulge.

Method

Phylogenetic analysis

Phylogenetic analyses were carried out in TNT V. 1.5 (Goloboff and Catalano 2016). The New Technology Search was applied first,

setting 10,000 Maximum trees, using sectorial searches, ratchet, drift, and tree fusing, and with the consensus stabilized 10 times. This yielded 18 trees of length 1217 steps. In order to reseach for additional topologies, the resulting 18MPTs were then used as the starting trees for a Traditional Search using TBR on the trees in RAM. The support for each node in the trees was assessed in TNT using GC values generated via symmetric resampling, based on 5000 replicates (Goloboff et al. 2003). The latter analyses used the Traditional Search option with TBR. Character mapping was carried out in Mesquite version 2.75 .

LSID

The electronic version of this article in Portable Document Format (PDF) will represent a published work according to the International Commission on Zoological Nomenclature (ICZN), and hence the new names contained in the electronic version are effectively published under that Code from the electronic edition alone. This published work and the nomenclatural acts it contains have been registered in ZooBank, the online registration system for the ICZN. The ZooBank LSIDs (Life Science Identifiers) can be resolved and the associated information viewed through any standard web browser by appending the LSID to the prefix http://zoobank.org/. The LSID for this publication is: urn:lsid:zoobank.org:pub:FB5F6854-40EC-4547-9624-A7099705525D. The online version of this work is archived and available from the following digital repositories: PeerJ, PubMed Central and CLOCKSS.

Acknowledgments

For their hospitality and access to specimens in their care, we wish to thank Luo JY, Yue SK, Yue SB, Wang H, Wang Q, and Pan SG . Ren Xin-Xin wishes to thank Dong ZM for his generous helping during the first research trip to Lufeng World Dinosaur Valley. We are grateful to C. Suarez (UARK) for helpful discussion and revision. Thoughtful reviews by anonymous reviewers, and the editor improved an earlier version of this manuscript.

Disclosure statement

No potential conflict of interest was reported by the authors.

Funding

This study is supported by grant from The Strategic Priority Research Program of Chinese Academy of Sciences (Grant number: XDB26000000) and National Natural Science Foundation of China (Grant numbers: 41688103, 41872021).

ORCID

Hai-Lu You http://orcid.org/0000-0003-2203-6461

References

Allain R, Aquesbi N. 2008. Anatomy and phylogenetic relationships of *Tazoudasaurus naimi* (Dinosauria, Sauropoda) from the late Early Jurassic of Morocco. Geodiversitas. 30(2):345–424.

Bandyopadhyay S, Gillette DD, Ray S, Sengupta DP. 2010. Osteology of *Barapasaurus tagorei* (Dinosauria: sauropoda) from the Early Jurassic of India. Palaeontology. 53(3):533–569. doi:10.1111/j.1475-4983.2010.00933.x.

Bonaparte JF. 1986. The early radiation and phylogenetic relationships of the Jurassic sauropod dinosaurs, based on vertebral anatomy. In: Padian K, editor. The Beginning of the Age of Dinosaurs. Cambridge: Cambridge University Press; p. 247–258.

Borsuk-Bialynicka M. 1977. A new camarasaurid sauropod *Opisthocoelicaudia skarzynskii* gen. n., sp. n., sp. n. from the Upper Cretaceous of Mongolia. Palaeontolo Polo. 37:1–80.

Calvo JO, Bonaparte JF. 1991. *Andesaurus delgadoi* gen et sp. nov. (Saurischia-Sauropoda) Dinosaurio Titanosauridae de la formacion Rio Limay (Albiano-Cenomaniano), Neuquen, Argentina. Ameghiniana. 28:303–310.

Carballido JL, Sander PM. 2013. Postcranial axial skeleton of *Europasaurus holgeri* (Dinosauria, Sauropoda) from the Upper Jurassic of Germany: implications for sauropod ontogeny and phylogenetic relationships of basal Macronaria. J Sys Palaeontolo. doi:10.1080/14772019.2013.764935.

Cooper MR. 1984. A reassessment of *Vulcanodon karibaensis* Raath (Dinosauria: saurischia) and the origin of the Sauropoda. Palaeont Afr. 25:203–231.

Cúneo R, Ramezani J, Scasso R, Pol D, Escapa I, Zavattieri AM, Bowring SA. 2013. High-precision U–Pb geochronology and a new chronostratigraphy for the Cañado´n Asfalto Basin, Chubut, central Patagonia: implications for terrestrial faunal and floral evolution in Jurassic. Gondwana Res. 24(3–4):1267–1275. doi:10.1016/j.gr.2013.01.010.

Curry-Rogers K, Forster CA. 2004. The skull of *Rapetosaurus krausei* (Sauropoda: titanosauria) from the Late Cretaceous of Madagascar. J Vertebr Paleontol. 24:121–144. doi:10.1671/A1109-10.

Dong ZM, Zhou SW, Zhang YH. 1983. Dinosaurs from the Jurassic of Sichuan. Palaeontolo Sin Ser C. 23:1–151.

Dong ZM, Zhou SW, Zhang YZ 1983. The Dinosaurian Remains from Sichuan Basin, China. In: Nanjing Institute of Geology and Palaeontology and Institute of Vertebrate Paleontology and Paleoanthropology Academia, editor. Palaeontologia Sinica. Beijing: Science Press; p. 1–151.

Fang XS, Pang QQ, Lu LW, Zhang ZX, Pan SG, Wang YM, Li XK, Cheng ZW 2000. Lower, Middle, and Upper Jurassic subdivision in the Lufeng region, Yunnan Province. Proceedings of the Third National Stratigraphical Conference of China, Beijing. 208–214.

Fang XS, Zhao XJ, Lu LW, Cheng ZW. 2004. Discovery of Late Jurassic *Mamenchisaurus* in Yunnan, southwestern China. Geolo Bull China. 23:1005–1009.

Gauthier J. 1986. Saurischian monophyly and the origin of birds. In: Padian K, editor. The Origin of Birds and the Evolution of Flight. Vol. 8. San Francisco: Memoirs of the California Academy of Sciences; p. 1–55.

Gilmore CW 1946. Reptilian fauna of the north Horn Formation of central Utah. United States Department of the Interior Geological Survey Professional Paper. 29–53.

Goloboff PA, Catalano SA. 2016. TNT version 1.5, including a full implementation of phylogenetic morphometrics. Cladistics Int J Willi Hennig Soc. 32:221–238. doi:10.1111/cla.12160.

Goloboff PA, Farris J, Kallersjö M, Oxelman B, Ramírez M, Szumik CA. 2003. Improvements to resampling measure of group support. Cladistics. 19:324–332. doi:10.1111/j.1096-0031.2003.tb00376.x.

Harris JD. 2006a. Cranial osteology of *Suuwassea emilieae* (Sauropoda: diplodocoidea: flagellicaudata) from the Upper Jurassic Morrison Formation of Montana, U.S.A. J Vertebr Paleontol. 26:88–102. doi:10.1671/0272-4634(2006)26[88:COOSES]2.0.CO;2.

He XL, Li C, Cai KJ. 1998. The Middle Jurassic Dinosaur Fauna from Dashanpu, Zigong, Sichuan: sauropod Dinosaurs, Volume 4, *Omeisaurus tianfuensis*. Chengdu: Sichuan Publishing House of Science and Technology; p. 1–143.

He XL, Yang SH, Cai KJ, Li K, Liu ZW. 1996. A new species of sauropod, *Mamenchisaurus anyuensis* sp. Nov. Proc 30th Int Geol Congr. 12:83–86.

Huang BC, Li YA, Fang XS, Sun DJ, Pang QQ, Cheng ZW, Li PX. 2015. Magnetostratigraphy of the Jurassic in Lufeng, central Yunnan. Geolo Bull China. 24:322–328.

Huang JD, You HL, Yang JT, Ren XX. 2014. A new sauropod dinosaur from the Middle Jurassic of Huangshan, Anhui Province. Vertebr Palasiat. 52:390–400.

Huene FV. 1932. Die Fossile Reptil-ordnung Saurischia: ihre Entwicklung und Geschichte. Gebruder Borntraeger. Monogr Geolo Palaontolo. S1:1–361.

Jacobs LL, Winkler DA, Downs WR, Gomani EM. 1993. New material of an Early Cretaceous titanosaurid sauropod dinosaur from Malawi. Palaeontology. 36:523–534.

Jiang S, Li F, Peng GZ, Ye Y. 2011. A new species of *Omeisaurus* from the Middle Jurassic of Zigong, Sichuan. Vertebr Palasiat. 39:185–194.

Lü JC, Kobayashi Y, Li TG, Zhong SM. 2010. A new basal sauropod dinosaur from the Lufeng Basin, Yunnan Province, southwestern China. Acta Geolo Sin (English Edition). 84(6):1336–1342. doi:10.1111/j.1755-6724.2010.00332.x.

Mannion PD, Upchurch P, Barnes RN, Mateus O. 2013. Osteology of the Late Jurassic Portuguese sauropod dinosaur *Lusotitan atalaiensis* (Macronaria) and the evolutionary history of basal titanosauriforms. Zool J Linn Soc. doi:10.1111/zoj.12029.

Mannion PD, Upchurch P, Schwarz DA, Wings O. 2019. Taxonomic affinities of the putative titanosaurs from the Late Jurassic Tendaguru Formation of Tanzania: phylogenetic and biogeographic implications for eusauropod dinosaur evolution. Zool J Linn Soc. 99:1–126.

Marsh OC. 1878. Principal characters of American Jurassic dinosaurs (Part 1). Am J Sci. 16:411–416. doi:10.2475/ajs.s3-16.95.411.

McIntosh JS, Miller WE, Stadtman KL, Gillette DD. 1996. The Osteology of *Camarasaurus lewisi* (Jensen, 1988). Byu Geolo Stud. 41:73–115.

McPhee BW, Upchurch P, Mannion PD, Corwin S, Butler RJ, Barrett PM. 2016. A revision of *Sanpasaurus yaoi* Young, 1944 from the Early Jurassic of China,

and its relevance to the early evolution of Sauropoda (Dinosauria). Peer J. doi:10.7717/peerj.2578.
Ouyang H. 1989. A new sauropod from Dashanpu, Zigong Co., Sichuan Province (*Abrosaurus dongpoensis* gen. et sp. nov.). Zigong Dinosaur Mus Newsl. 2:10–14.
Ouyang H, Ye Y. 2002. The first mamenchisaurian skeleton with complete skull *Mamenchisaurus youngi*. Chengdu: Sichuan Publishing House of Science and Technology; p. 1–111.
Owen R. 1842. Report on British Fossil Reptiles. Part II. Rep Br Assoc Adv Sci. 11:60–204.
Peng GZ, Ye Y, Gao YH, Shu CK, Jiang S. 2005. Jurassic Dinosaur Faunas in Zigong. Chengdu: Sichuan People's Publishing House; p. 236.
Pi LZ, Ouyang H, Ye Y 1996. A new species of sauropod from Zigong, Sichuan: *mamenchisaurus youngi*. In: Department of Spatial Planning and Regional Economy, editor. Geosciences from the 30th International Geological Congress. Beijing: China Economic Publishing House; p. 87–91.
Poropat SF, Mannion PD, Upchurch P, Hocknull SA, Kear BP, Elliott DA. 2014. Reassessment of the non-Titanosaurian somphospondylan *Wintonotitan wattsi* (Dinosauria: sauropoda: titanosauriformes) from the Mid-Cretaceous Winton Formation, Queensland, Australia. Palaeontology. 1–48.
Poropat SF, Mannion PD, Upchurch P, Hocknull SA, Kear BP, Kundrat M, Tischler TR, Sloan T, Sinapius GHK, Elliott JA, et al. 2016. New Australian sauropods shed light on Cretaceous dinosaur palaeobiogeography. Sci Rep. doi:10.1038/srep34467.
Powell JE. 1992. Osteología de Saltasaurus Loricatus (Sauropoda-Titanosauridae) del Cretácico Superior argentino. In: Sanz JL, Buscalioni AD, editors. Los dinosaurios y su entorno biótico II Curso de Paleontología, 10 a 12 de julio de 1990 Actas. Cuenca: Instituto Juan de Valdés, Serie Actas Academicas; p. 165–230.
Remes K. 2006. Revision of the Tendaguru sauropod dinosaur Tornieria africana (Fraas) and its relevance for sauropod paleobiogeography. J Vertebr Paleontol. 26:651–669. doi:10.1671/0272-4634(2006)26[651:ROTTSD]2.0.CO;2.
Ren XX, Huang JD, You HL. 2018. The second mamenchisaurid dinosaur from the Middle Jurassic of Eastern China. Hist Biol. doi:10.1080/08912963.2018.1515935.
Royo-Torres R, Cobos A, Alcala L. 2006. A giant European dinosaur and a new sauropod clade. Science. 314:1925–1927. doi:10.1126/science.1132885.
Salgado L, Bonaparte JF. 1991. Un nuevo sauropodo Dicraeosauridae, *Amargasaurus cazaui* gen. et sp. nov., de la Formacion La Amarga, Neocomiano de la Provincia del Neuquen, Argentina. Ameghiniana. 28:333–346.
Salgado L, Coria RA, Calvo JO. 1997. Evolution of Titanosaurid sauropods. I: phylogenetic analysis based on the postcranial evidence. Ameghiniana. 34:3–32.
Seeley HG 1887. On the classification of the fossil animals commonly named Dinosauria. Proceedings of the Royal Society of London. 43: 165–171.
Sekiya T. 2011. Re-examination of *Chuanjiesaurus anaensis* (Dinosauria: sauropoda) from the Middle Jurassic Chuanjie Formation, Lufeng Country, Yunnan Province, Southwest China. Mem Fukui Prefectural Dinosaur Mus. 10:1–54.
Sekiya T, Dong ZM. 2010. A new juvenile specimen of *Lufengosaurus huenei* Young, 1941 (Dinosauria: prosauropoda) from the Lower Jurassic Lower Lufeng Formation of Yunnan, southwest China. Acta Geolo Sin (English Edition). 84(1):11–21. doi:10.1111/j.1755-6724.2010.00165.x.
Sereno PC, Wilson JA, Witmer LM, Whitlock J, Maga AA, Ide O, Rowe TA. 2007. Structural extremes in a Cretaceous dinosaur. PLoS One. 2:e1230. doi:10.1371/journal.pone.0001230.
Tan C, Dai H, He JJ, Zhang G, Hu XF, Yu HD, Li N, Wei GB, Peng GZ, Ye Y, et al. 2018. Discovery of Omeisaurus (Dinosauria: sauropoda) in the Middle Jurassic Shaximiao Formation of Yunyang, Chongqing, China. Vertebr Palasiat. doi:10.19615/j.cnki.1000-3118.181115.
Tang F, Jing X, Kang X, Zhang G. 2001. *Omeisaurus maoianus*: A Complete Sauropod from Jingyan, Sichuan. Beijing: China Ocean Press; p. 1–128.
Taylor M. 2009. A re-evaluation of *Brachiosaurus altithorax* Riggs 1903 (Dinosauria, Sauropoda) and its generic separation from *Giraffatitan brancai* (Janensch 1914). J Vertebr Paleontol. 29:787–806. doi:10.1671/039.029.0309.
Tschopp E, Mateus OBenson RBJ. 2015. A specimen-level phylogenetic analysis and taxonomic revision of diplodocidae (dinosauria, sauropoda). Peerj. 3: e857. doi:
Upchurch P. 1995. The evolutionary history of sauropod dinosaurs. Philos Trans R Soc London. 349:365–390.
Upchurch P. 1998. The phylogenetic relationships of sauropod dinosaurs. Zool J Linn Soc. 124:43–103. doi:10.1111/j.1096-3642.1998.tb00569.x.
Upchurch P, Barrett PM, Dodson P. 2004. Sauropoda. In: Weishampel DB, Dodson P, Osmólska H, editors. The Dinosauria.. *Second* ed. Berkeley: University of California Press; p. 259–322.
Upchurch P, Barrett PM, Galton PM. 2007a. A phylogenetic analysis of basal sauropodomorph relationships: implications for the origin of sauropod dinosaurs. Spec Pape Palaeontol. 77:57–90.
Upchurch P, Martin J. 2003. The anatomy and taxonomy of *Cetiosaurus* (Saurischia, Sauropoda) from the Middle Jurassic of England. J Vertebr Paleontol. 23(1):208–231. doi:10.1671/0272-4634(2003)23[208:TAATOC]2.0.CO;2.
Wang YM, You HL, Wang T. 2017. A new basal sauropodiform dinosaur from the Lower Jurassic of Yunnan Province, China. Sci Rep. doi:10.1038/srep41881.
Whitlock JA, Harris JD. 2010. The dentary of *Suuwassea emilieae* (Sauropoda: diplodocoidea). J Vertebr Paleontol. 30:1637–1641. doi:10.1080/02724634.2010.501452.
Wilson JA, Sereno PC. 1998. Early evolution and higher level phylogeny of sauropod dinosaurs. Soci Vertebr Paleontolo Mem. 5:1–68. doi:10.2307/3889325.
Wilson JA, Upchurch P. 2003. A revision of *Titanosaurus lydekker* (Dinosauria-Sauropoda), the first dinosaur genus with a 'Gondwanan' distribution. J Syst Paleontol. 1:125–160. doi:10.1017/S1477201903001044.
Xing LD, Miyashita T, Currie PJ, You HL, Zhang JP, Dong ZM. 2015b. A new basal eusauropod from the Middle Jurassic of Yunnan, China, and faunal compositions and transitions of Asian sauropodomorph dinosaurs. Acta Palaeontol Pol. 60(1):145–154. doi:10.4202/app.2012.0151.
Xu X, Upchurch P, Mannion PD, Barrett PM, Regalado- Fernandez OR, Mo JY, Ma J, Liu HG. 2018. A new Middle Jurassic diplodocoid suggests an earlier dispersal and diversification of sauropod dinosaurs. Nat Commun. doi:10.1038/s41467-018-05128-1.Yates.
Yates AM, Kitching JW. 2003. The earliest known sauropod dinosaur and the first steps towards sauropod locomotion. Proc R Soc B. 270(1525):1753–1758. doi:10.1098/rspb.2003.2417.
Young CC. 1939. On a new Sauropoda, with notes on other fragmentary reptiles from Szechuan. Bull Geol Soc China. 19:235–279.
Young CC. 1941. A complete osteology of *Lufengosaurus huenei* Young (gen. et sp. nov.) from Lufeng, Yunnan, China. Palaeontolo Sin Ser C. 7:1–53.
Young CC. 1942. *Yunnanosaurus huangi* Young (gen. et sp. nov.), a new Prosauropoda from the Red Beds at Lufeng, Yunnan. Bull Geol Soc China. 22(1–2):63–104.
Young CC. 1947. On *Lufengosaurus magnus* Young (sp. nov.) and additional finds of *Lufengosaurus huenei* Young. Palaeontolo Sin Ser C. 12:1–53.
Young CC. 1948. Further notes on *Gyposaurus sinensis* Young. Bull Geol Soc China. 28(1–2):91–103.
Young CC. 1951. The Lufeng saurischian fauna in China. Palaeontolo Sin Ser C. 13:1–94.
Young CC, Chao XJ. 1972. Mamenchisaurus hochuanensis. In: editor. Institute of Vertebrate Paleontology and Paleoanthropology Monograph Series I. Beijing: Science Press; p. 1–30.
Zhang QN, You HL, Wang T, Chatterjee S. 2018. A new sauropodiform dinosaur with a 'sauropodan' skull from the Lower Jurassic Lufeng Formation of Yunnan Province, China. Sci Rep. doi:10.1038/s41598-018-31874-9.
Zhang YH. 1988. The Middle Jurassic Dinosaur Fauna from Dashanpu, Zigong, Sichuan: sauropod Dinosaurs, Volume 3, *Shunosaurus lii*. Chengdu: Sichuan Publishing House of Science and Technology; p. 1–89.
Zhang YH, Li K, Zeng QH. 1998. A new species of sauropod dinosaur from the Upper Jurassic of Sichuan Basin, China. J Chengdu Univ Technol. 25:60–70.
Zhang YH, Yang ZL. 1995. A new complete osteology of Prosauropoda in Lufeng Basin, Yunnan, China: *jingshanosaurus*. Kunming: Yunnan Publishing House of Science and Technology; p. 1–90.